https://doi.org/10.5194/egusphere-2025-4000
Preprint. Discussion started: 29 September 2025

Ocean dynamics amplify remote warming effects of reforestation

Pierre Etienne Banville[1], Alexander J. MacIsaac[1,2], Kirsten Zickfeld[1]

[1]Department of Geography, Simon Fraser University, Burnaby, V5A 1S6, Canada
[2]Department of Earth and Environmental Sciences, St. Francis Xavier University, Antigonish, B2G 2W5, Canada

Correspondence to: Pierre Etienne Banville (peb1@sfu.ca)

Abstract. Forestation, including reforestation, afforestation, and forest restoration, is prevalent in net-zero climate strategies due to the large carbon sequestration potential of forests. In addition to capturing carbon, forestation has biogeophysical effects that can influence surface temperatures locally (local effects), and at distant locations (non-local effects). Biogeophysical effects may offset the cooling benefits of carbon sequestration, hence requiring a robust understanding of their mechanisms to adequately integrate forestation into climate mitigation strategies. Yet, the role of ocean dynamics, such as ocean circulation, ocean-atmosphere interactions, and ocean-sea ice interactions in mediating the non-local effects of forestation remains underexplored. In this study, we investigate the impact of ocean dynamics on the magnitude and geographic patterns of the non-local biogeophysical effects of large-scale reforestation, with the exclusion of cloud feedbacks, over a multi-century timescale using the University of Victoria Earth System Climate Model. We conduct multi-century paired global reforestation simulations, with the first set of simulations using a dynamic ocean and the second set using prescribed sea surface temperatures. We separate local from non-local effects using the checkerboard approach. Our results show that non-local warming effects are of much greater magnitude and encompass a greater geographic area, particularly at high latitudes, when ocean dynamics are considered. Moreover, this study shows that ocean dynamics introduce a lag in the non-local effects, leading to a continued increase in non-local warming even after the local effects have stabilized. This committed non-local warming is driven by the thermal inertia of the ocean, which sustains a gradual long-term increase in sea surface temperatures, combined with amplifying climate feedbacks. Decision-making frameworks must therefore consider the complete Earth system response to forestation over a sufficiently long timeframe to account for the committed non-local warming.

1. Introduction

Forestation, referring to afforestation (planting trees on land that has been unforested for 50 years or more), reforestation (planting trees on land that has been unforested for less than 50 years), and forest restoration (repairing degraded forests), is a prevalent strategy in climate change mitigation pathways and policies aiming to achieve net-zero emissions before the end of this century due to the carbon sequestration potential of forests (Cook-Patton et al., 2020; Minx et al., 2018; Mo et al., 2023; Riahi et al., 2022; Roe et al., 2019; Smith et al., 2022). This attribute of forests, combined with their provision of ecosystem services, has given rise to large-scale forestation initiatives, such as the UN Decade on Ecosystem Restoration and the Bonn Challenge in which 115 countries have committed to restore 1000 Mha of land by 2040 (Sewell et al., 2020). Underlying the use of forestation in net-zero strategies is

https://doi.org/10.5194/egusphere-2025-4000
Preprint. Discussion started: 29 September 2025

the assumption that a fossil fuel CO_2 emission in the atmosphere can be balanced by removing an equivalent amount via carbon sequestration in trees. However, forestation impacts the Earth system in ways that go beyond carbon sequestration, resulting in a different climate outcome than avoiding the fossil fuel emission (Zickfeld et al., 2023). For instance, forestation alters properties and processes at the land surface, such as surface albedo, surface roughness, and evapotranspiration rates, resulting in a change in the surface energy balance (Betts, 2000; Betts et al., 2007; Bonan, 2008; Winckler et al., 2019a). While these biogeophysical effects have received significant attention (Bonan, 2008; De Hertog et al., 2023; Pongratz et al., 2021; Smith et al., 2016), the role of ocean dynamics in mediating their propagation and driving temperature changes in distant regions remains underexplored. A robust quantification and understanding of the global Earth system impacts of forestation is needed for adequately integrating forestation into climate strategies and decision-making frameworks.

Biogeophysical effects can impact surface temperatures both at the location of forestation ("local effects") and at distant locations ("non-local effects") (Winckler et al., 2017). Quantifying non-local biogeophysical effects is challenging because these effects cannot be captured by direct observations and can only be determined by climate modeling studies (Pongratz et al., 2021; Winckler et al., 2019b). Most global modeling studies of large-scale forestation (or deforestation) suggest a non-local global warming (or cooling in the case of deforestation), more pronounced at high latitudes due to the snow-masking effect of forests (Arora and Montenegro, 2011; Boysen et al., 2020; Chen and Dirmeyer, 2020; De Hertog et al., 2023; Devaraju et al., 2018; Liu et al., 2023; Winckler et al., 2019b). However, regional results vary significantly between models and can even be contradictory (Boysen et al., 2020; De Hertog et al., 2023; Liu et al., 2023). Moreover, many studies have focused only on land-atmosphere interactions (Chen et al., 2022; Chen and Dirmeyer, 2020; Devaraju et al., 2018; Liu et al., 2023; Noblet-Ducoudré et al., 2012), potentially underestimating the magnitude of non-local effects as oceanic processes can play a significant role in propagating and amplifying biogeophysical effects (Davin and Noblet-Ducoudré, 2010; Winckler et al., 2019b).

Forestation can lead to an increase in Sea Surface Temperature (SST) due to the advection of warmer and wetter air from the land to the ocean (Wang et al., 2014). This increase in SST can trigger a weakening of the Atlantic Meridional Overturning Circulation (AMOC) by decreasing the density of surface water (Portmann et al., 2022; Wang et al., 2014; Weaver et al., 2012). Such a weakening of the AMOC reduces meridional oceanic heat transport and increases upper oceanic heat content (with the exception of the North Atlantic warming hole region) (Portmann et al., 2022). A reduced meridional heat transport can reduce Arctic sea ice loss and slow down Arctic warming, acting as a negative feedback (Liu et al., 2020). On sufficiently long timescales, changes in oceanic heat transport can lead to further changes in SST, influencing energy fluxes between the ocean and the atmosphere (Buckley and Marshall, 2016). Moreover, ocean-atmosphere interactions can strengthen the initial SST warming via the water vapor feedback and the sea ice-albedo feedback (Ganopolski et al., 2001). Ocean dynamics, such as ocean circulation, ocean-atmosphere interactions, and ocean-sea ice interactions, can therefore alter remote temperature patterns well beyond the local area of forestation.

https://doi.org/10.5194/egusphere-2025-4000
Preprint. Discussion started: 29 September 2025

Studies investigating the effects of ocean dynamics in mediating the biogeophysical effects of forestation on Land Surface Temperature (T_{surf_land}) or Surface Air Temperature (T_{air}) are limited. Regional forestation studies of the Southern Hemisphere and East China found that ocean dynamics lead to a slight amplification in T_{air} warming due to the water vapor feedback (Ma et al., 2013; Wang et al., 2015). Similarly, deforestation studies found that ocean dynamics either convert a global warming signal from deforestation into a global cooling signal or intensify a global cooling signal in the case of boreal deforestation due to water vapor and sea ice-albedo feedbacks (Davin and Noblet-Ducoudré, 2010; Ganopolski et al., 2001). However, all of these studies, with the exception of the deforestation study by Ganopolski et al. (2001), were regional and performed on relatively short timeframes of up to 110 years, which does not allow for the full ocean response (Li et al., 2013). As a result, the role of ocean dynamics in influencing the non-local biogeophysical effects of large-scale global forestation over a multi-century timescale remains unknown. Such knowledge could facilitate the integration of the full Earth system impacts of large-scale forestation in decision-making frameworks by revealing the temporal dynamics of the non-local effects.

In this study, we investigate the role of ocean dynamics in mediating the non-local biogeophysical effects of large-scale global forestation on T_{surf_land}. More specifically, we answer the following questions: 1) what is the impact of ocean dynamics on the magnitude and geographic patterns of the non-local biogeophysical effects on a multi-century timescale, and 2) how do ocean dynamics influence these non-local effects. We isolate the impact of ocean dynamics from a set of multi-century global large-scale forestation simulations using the University of Victoria Earth System Climate Model (UVic ESCM). We first provide an overview of the local and non-local biogeophysical effects of global forestation at the time when vegetation has regrown. We then compare the non-local effects with and without ocean dynamics at that same point in time and discuss the underlying physical mechanisms leading to the differences. Finally, we examine how the non-local effects evolve over time with and without ocean dynamics and contrast this temporal evolution with that of the local effects. These results provide insights into the role of ocean dynamics in propagating the non-local biogeophysical effects of forestation and into the relative magnitude of the local and non-local effects at different points in time. These findings can have important implications for decision-making frameworks considering large-scale forestation as a climate mitigation strategy.

2. Methods

2.1 Model description

We used the University of Victoria Earth System Climate Model (UVic ESCM) version 2.10 (Mengis et al., 2020; Weaver et al., 2001) to perform simulations. The UVic ESCM is an Earth System Model of intermediate complexity with a resolution of 1.8 degrees latitude by 3.6 degrees longitude (Mengis et al., 2020). The atmosphere is represented by a single-layer energy-moisture balance model, in which heat and moisture are transported between grid cells via advection and diffusion (Weaver et al., 2001). Given the simplified atmosphere, the UVic ESCM does not represent cloud feedbacks nor atmospheric dynamics. The ocean component is based on the Geophysical Fluid Dynamics Laboratory (GFDL) Modular Ocean Model (MOM) version 2 (Weaver et al., 2001). It has 19 layers which follow a parabolic profile, from 50m at the surface to 518m at the deepest level. Ocean surface dynamics are

https://doi.org/10.5194/egusphere-2025-4000
Preprint. Discussion started: 29 September 2025

driven by both wind stress and surface buoyancy forcing. The ocean component is coupled to a thermodynamic-dynamic sea ice model (Bitz et al., 2001).

On land, vegetation dynamics are based on the Dynamic Global Vegetation Model TRIFFID (Top-down Representation of Interactive Foliage and Flora Including Dynamics) which allows for five plant functional types (PFTs; broadleaf and needleleaf trees, C3 and C4 grasses, and shrubs) to compete for space based on Lotka–Volterra equations (Cox, 2001). The subsurface has 14 layers: 8 hydrologically active soil layers where freeze-thaw processes are resolved and 6 bedrock layers (Mengis et al., 2020). The UVic ESCM contains a full representation of the global carbon cycle, including a multi-layer soil carbon representation and an organic and inorganic ocean carbon cycle (Mengis et al., 2020). In this fully-coupled arrangement, the UVic ESCM can be used to determine changes in Earth system attributes, such as T_{surf_land} and SST, resulting from changes in land cover.

Changes in land cover is represented by constraining the PFTs that are allowed to grow on a given grid cell. More specifically, deforestation is represented by prescribing a land-cover map that allows for the growth of only C3 and C4 grasses in deforested grid cells. Reforestation can be represented by removing the PFT constraints, allowing for shrubs, needleleaf trees and broadleaf trees to regrow on grid cells that have been previously deforested. The dominant PFT in each grid cell depends on growth and competition dynamics.

2.2 Model experiments

The model was spun up over 10,000 years to establish a climate in equilibrium with pre-industrial forcings – including non-CO_2 radiative forcing, and atmospheric CO_2 concentration, as described in CMIP6 protocols (Eyring et al., 2016). There were however no constraints on land cover in this spin-up, allowing all PFTs to grow freely. From the spin-up, we performed a global deforestation simulation by allowing the growth of only C3 and C4 grasses on land and keeping CO_2 concentration and other forcings constant at pre-industrial level ("Deforestation Simulation"). Keeping CO_2 concentration and other forcings constant allows us to isolate the biogeophysical effects of land cover changes. We let this simulation run for 1500 years to stabilize surface temperature (**Fig. A1a**).

From the end of the Deforestation Simulation, we performed a set of idealized reforestation simulations ("Reforestation Simulations"), as shown in **Table 1**. To achieve reforestation on a given grid cell, we instantaneously removed the constraints associated with PFTs discussed in the prior section. After 500 years, the Reforested State is reached (**Fig. 1**), a state where the growth of shrubs, needleleaf trees, and broadleaf trees has stabilized and vegetation has largely recovered to its pre-deforestation state (**Fig. A1b**). We used the checkerboard approach described in Winckler et al. (2017) to alternate grid cells that remain deforested with grid cells that are subject to reforestation to be able to isolate local effects from non-local effects (**Fig. A2**). We varied the extent of reforestation as occurring on either 50% or 25% of land grid cells.

To determine the impact of ocean dynamics on the biogeophysical effects of forestation, we ran simulations with a dynamic ocean ("Dynamic Ocean Simulations") and simulations with prescribed SST ("Prescribed SST Simulations"). In the Prescribed SST Simulations, ocean circulation is absent, and ocean-atmosphere interactions

https://doi.org/10.5194/egusphere-2025-4000
Preprint. Discussion started: 29 September 2025

and ocean-sea ice interactions are based on fixed SST, preventing any feedback. On the other hand, in the Dynamic Ocean Simulations, ocean circulation, ocean-atmosphere interactions and ocean-sea ice interactions respond freely to changes in the Earth system. In the Prescribed SST Simulations, the SST of each ocean grid cell was set based on the 5-day average SST from the last 100 years of the Deforestation Simulation. Therefore, SST stayed the same each year but changed every 5 days to reflect variations over the course of one year. All Reforestation Simulations were run for over 1,000 years.

Table 1: Description of Reforestation Simulations

Name	**Percentage of reforested grid cells**	**Treatment of Sea Surface Temperature**
Dynamic Ocean Simulation	50%	Dynamic
Prescribed SST Simulation	50%	Prescribed
Dynamic Ocean Simulation-25%	25%	Dynamic
Prescribed SST Simulation-25%	25%	Prescribed

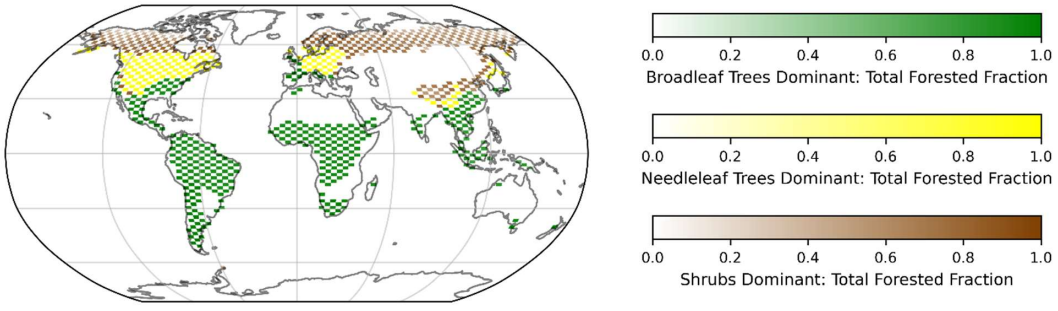

Figure 1: Global reforestation extent when the Reforested State is reached following reforestation of 50% of grid cells. Green grid cells represent grid cells where broadleaf trees are the dominant species. Yellow grid cells represent grid cells where needleleaf trees are the dominant species. Brown grid cells represent grid cells where shrubs are the dominant species. For each grid cell, the color intensity represents the total fraction of grid cell that has been reforested by all types of trees combined (broadleaf trees, needleleaf trees, and shrubs). In each grid cell, the dominant species represents the PFT with the highest areal fraction.

2.3 Analysis: Separation of local and non-local effects

To investigate the role of ocean dynamics on the non-local biogeophysical effects, we first need to distinguish between local and non-local effects on T_{surf_land} in the Reforestation Simulations. To do so, we compared the value of T_{surf_land} in the Reforestation Simulations with its value in the Deforestation Simulation following the procedure described in Winckler et al. (2017). Over reforested grid cells, the difference in T_{surf_land} between the

https://doi.org/10.5194/egusphere-2025-4000
Preprint. Discussion started: 29 September 2025

Reforestation Simulations and the Deforestation Simulation represents the total (local + non-local) effect, whereas over grid cells that remained deforested, the difference represents only the non-local effect.

To separate local from non-local effects over reforested grid cells, we first latitudinally interpolated the non-local effect between deforested grid cells to get a global map of non-local effects. We then subtracted the non-local effect from the total effect over reforested grid cells to obtain the local effects. For all calculations, temperatures were averaged over 25 years to smooth out internal climate variability. We performed the separation of local and non-local biogeophysical effects when the Reforested State is reached, and 500 years afterwards to determine their changes over time. In addition to determining local and non-local effects on T_{surf_land}, we also isolated local and non-local effects on T_{air}. In the UVic ESCM, T_{air} is defined as the sea level air temperature determined from the vertically-integrated atmospheric energy balance equation (Weaver et al., 2001). It is therefore less tightly coupled to T_{surf_land} than in other Earth System Models. Results related to T_{air} are shown in Appendix A.

2.4 Analysis: Surface energy balance decomposition

To gain a better understanding of the drivers of the local and non-local effects and of the role of ocean dynamics in mediating the non-local effects, we decomposed the change in T_{surf_land} into contributions from the individual terms of the surface energy balance. This method is widely used to analyze the biogeophysical effects of land use change (Boysen et al., 2020; De Hertog et al., 2023; Winckler et al., 2017). The surface energy budget is balanced between the net incoming shortwave radiation (SW_{net}), the net incoming longwave radiation (LW_{net}), the latent heat flux (LE), the sensible heat flux (H), and the ground heat flux (G), as per **Eq. (1)**. Due to the long timescales involved, we can assume that energy storage is zero.

$$SW_{net} + LW_{net} = LE + H + G \quad (1)$$

Applying the Stefan-Boltzmann law and taking the total derivative with respect to T_{surf_land}, we obtain:

$$\Delta T_{surf\_land} = \frac{1}{4\sigma * \varepsilon * T_{surf\_land}^{3}} * (\Delta SW_{net} + \Delta LW_{down} - \Delta LE - \Delta H - \Delta G) \quad (2)$$

where σ is the Stefan–Boltzmann constant and ε is emissivity and is set to 0.97

For all Reforestation Simulations, we first decomposed the total difference in T_{surf_land} between the Reforestation Simulation and the Deforestation Simulation into the individual terms of the surface energy balance using **Eq. (2)**. As changes in ground heat flux are marginal following reforestation, we omitted the term ΔG in the analysis (Winckler et al., 2017).

To be able to perform the surface energy balance decomposition for the local and non-local effects, we then split the individual components of the surface energy balance (SW_{net}, LW_{down}, LE, and H) into local and non-local components following the checkerboard procedure described in the previous section. We subsequently decomposed the difference in T_{surf_land} between the Reforestation Simulation and the Deforestation Simulation caused by non-local effects ($\Delta T_{surf\_land\_nonlocal}$) and local effects ($\Delta T_{surf\_land\_local}$) into the non-local components of the surface energy balance (**Eq. (3)**) and the local components of the surface energy balance respectively (**Eq. (4)**). For all surface

https://doi.org/10.5194/egusphere-2025-4000
Preprint. Discussion started: 29 September 2025

energy balance decompositions, we used the same timeframes that were used to separate local and non-local effects previously.

$$\Delta T_{surf\_land\_nonlocal} = \frac{1}{4\sigma * \varepsilon * T_{surf\_land}^{3}} * \left(\Delta SW_{net\_nonlocal} + \Delta LW_{down\_nonlocal} - \Delta LE_{nonlocal} - \Delta H_{nonlocal}\right) \quad (3)$$

$$\Delta T_{surf\_land\_local} = \frac{1}{4\sigma * \varepsilon * T_{surf\_land}^{3}} * \left(\Delta SW_{net\_local} + \Delta LW_{down\_local} - \Delta LE_{local} - \Delta H_{local}\right) \quad (4)$$

3. Results

3.1 Local cooling and non-local warming effects

The biogeophysical effects of reforestation of 50% of grid cells on temperature when the Reforested State is reached are a global warming of SST, a global warming of T_{surf_land} at high latitudes and a cooling of T_{surf_land} in the Tropics (**Fig. 2**). These changes in surface temperature stem from the combination of local cooling and non-local warming effects (**Fig. 2**). At high latitudes, where shrubs are dominant, the local effects are small and are more than offset by the non-local warming effects. In the Tropics, where broadleaf trees are dominant, the local cooling effects are much stronger and overpower the non-local warming effects. Areas dominated by needleleaf trees, such as mid-latitude North America and Europe, experience either mild warming or mild cooling, with the cooling strengthening as we move southwards. Non-reforested areas, such as mid-latitude Asia, are dominated by the non-local warming effects.

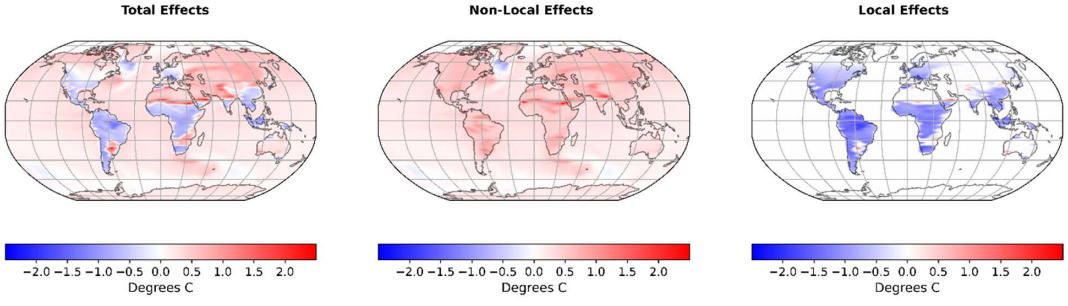

Figure 2: Total, non-local, and local biogeophysical effects of reforestation of 50% of grid cells on surface temperature (T_{surf_land} and SST) when the Reforested State is reached in the Dynamic Ocean Simulation. Maps of local effects show the local effects on reforested grid cells and their interpolation to non-reforested grid cells. The total effects are the sum of the local effects (including interpolated local effects) and the non-local effects.

Changes in land surface properties due to reforestation lead to a decrease in T_{surf_land} locally, more pronounced in the Tropics. Reforestation leads to a decrease in surface albedo in the impacted areas, increasing the net incoming shortwave radiation (**Fig. A3**). Reforestation also leads to a decrease in evapotranspiration over land, decreasing the latent heat flux (**Fig. A3**). As the decrease in latent heat flux is contrary to most models (**Fig. B2a**), we discuss implications of this result in Section 4. Finally, reforestation also increases the upward sensible heat flux,

https://doi.org/10.5194/egusphere-2025-4000
Preprint. Discussion started: 29 September 2025

compensating for the reduction in latent heat flux to maintain the surface energy balance (**Fig. A3**). Changes in the net incoming longwave radiation are negligible (**Fig. A3**). The combination of these local factors leads to a local cooling of T_{surf_land} since the local increase in sensible heat flux more than offsets the local decrease in latent heat flux and the local increase in net incoming shortwave radiation (**Fig. 3,** Local Effects). Local effects are more pronounced in the Tropics due to the presence of trees with a greater Leaf Area Index (broadleaf trees, as opposed to needleleaf trees and shrubs at high latitudes), which enhances energy fluxes differences.

The non-local warming effects arise from the local increases in sensible heat flux and net incoming shortwave radiation, which lead to an increase in T_{air}. The warmer air is advected away from reforested areas, as reflected in the global increase in T_{air} (**Fig. A4**). This increase in air temperature contributes to increasing the water vapor capacity of the atmosphere, as a result of the Clausius-Clapeyron relationship. The increased water vapor capacity of the atmosphere leads to an increase in the water vapor content of the atmosphere (**Fig. A5**) despite the decrease in evapotranspiration (**Fig. A6**). The increase in water vapor in the atmosphere strengthens the greenhouse effect, leading to an increase in incoming longwave radiation globally. This non-local increase in incoming longwave radiation leads to non-local warming globally (**Fig. 3,** Non-Local Effects), increasing SST and T_{surf_land}. Feedbacks triggered by ocean dynamics, which are described in the next section, amplify the non-local warming effects.

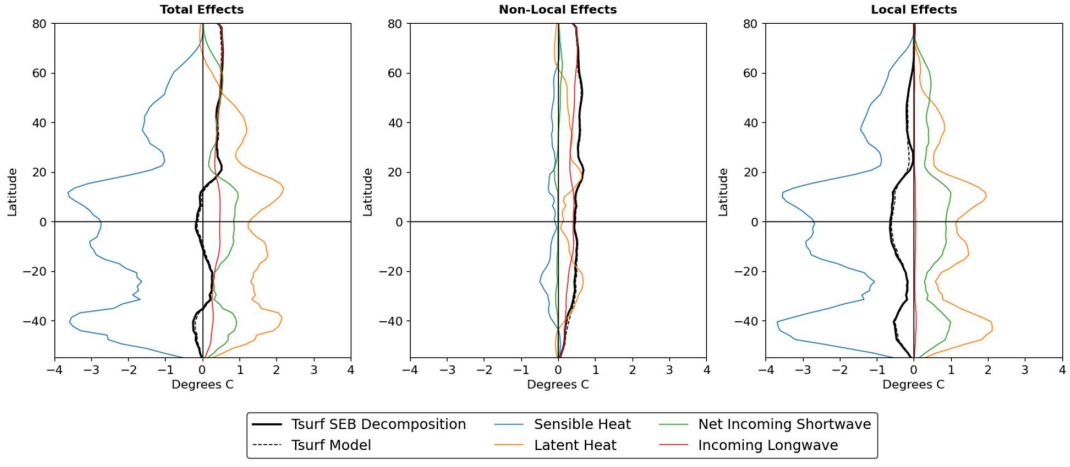

Figure 3: Surface Energy Balance decomposition of total, non-local, and local biogeophysical effects over land when the Reforested State is reached following reforestation of 50% of grid cells in the Dynamic Ocean Simulation. To account for reforestation of 50% of grid cells, local effects are averaged over both reforested and non-reforested cells (where local effects are zero). The total effects are the sum of the non-local effects and of the local effects. All values are latitudinally averaged over land areas.

https://doi.org/10.5194/egusphere-2025-4000
Preprint. Discussion started: 29 September 2025

3.2 Ocean dynamics amplify non-local warming effects

The role of ocean dynamics in amplifying the non-local effects is substantial. The non-local warming effects on T_{surf_land} are of much greater magnitude and encompass a greater geographic area in the Dynamic Ocean Simulation compared to the Prescribed SST Simulation (**Fig. 4**). A similar pattern is seen with T_{air} (**Fig. A7**). The advection of warmer and moister air across the globe and redistribution of heat by ocean circulation lead to a global increase in SST. The increase in SST is then amplified and further increases T_{surf_land} and T_{air} through a combination of feedbacks, particularly pronounced at high latitudes.

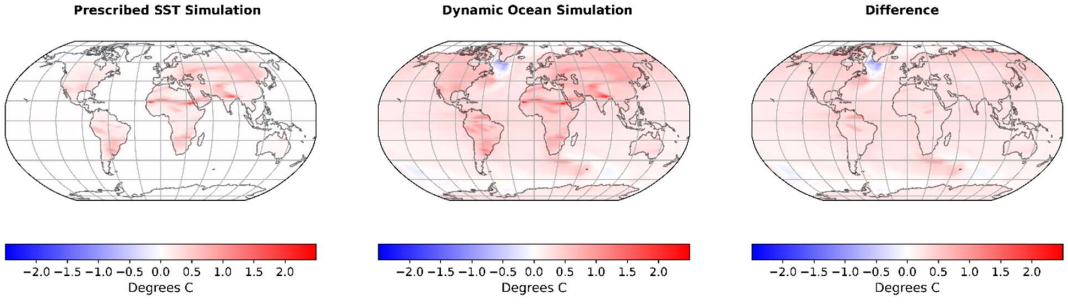

Figure 4: Non-local biogeophysical effects of reforestation of 50% of grid cells on surface temperature (T_{surf_land} and SST) when the Reforested State is reached in the Prescribed SST Simulation and in the Dynamic Ocean Simulation, and difference between the non-local effects of these two simulations (Dynamic Ocean Simulation minus Prescribed SST Simulation).

Firstly, the increase in SST amplifies the water vapor feedback. The increase in SST increases evaporation over the ocean (**Fig. A6c**), increasing the amount of water vapor over the ocean. This additional water vapor is redistributed globally through advection. Such increase in the water vapor content of the atmosphere strengthens the greenhouse effect and increases the incoming longwave radiation, which further increases SST, T_{surf_land} and T_{air} globally. In addition, the increase in T_{air} further increases the water vapor capacity of the atmosphere. Compared to the Prescribed SST Simulation, the water vapor feedback is stronger in the Dynamic Ocean Simulation due to a greater evaporative flux to the atmosphere and an increase in water vapor capacity, both contributing to increasing the amount of water vapor in the atmosphere globally (**Fig. A5**). As a result, in the Dynamic Ocean Simulation, the increase in incoming longwave radiation due to the water vapor feedback drives most of the non-local warming effect, whereas it has a more modest contribution to the non-local warming effect in the Prescribed SST Simulation (**Fig. 5**, red line).

Secondly, the increase in SST contributes to the sea ice-albedo feedback. The increase in SST at high latitudes causes a reduction in sea ice (**Fig. A8**), reducing surface albedo and increasing the net incoming shortwave radiation at high latitudes (**Fig. A3,** net incoming shortwave radiation). This increase in incoming shortwave radiation increases SST, T_{surf_land} and T_{air}, further reducing sea ice. The greater increase in T_{air} at high latitudes (**Fig. A7**) confirms the influence of this feedback in strengthening the warming at high latitudes. Moreover, the sea ice-albedo feedback and the water vapor feedback reinforce each other, both contributing to further increases in SST,

https://doi.org/10.5194/egusphere-2025-4000
Preprint. Discussion started: 29 September 2025

T_{surf_land}, and T_{air} at high latitudes. The water vapor feedback is more pronounced at high latitudes, as shown by the greater increase in incoming longwave radiation at high latitudes (**Fig. 5,** red line).

Finally, the non-local increase in temperature at high latitudes triggers a temperature-vegetation feedback. An increase in temperature increases the total Leaf Area Index both in grid cells that have been reforested and in grid cells that remained deforested (**Fig. A9**). This leads to a decrease in albedo, increasing the net incoming shortwave radiation at high latitudes, which further increases T_{surf_land} and T_{air}. The impact of this feedback can be seen by the small positive contribution of the net incoming shortwave radiation in the surface energy balance decomposition of non-local effects (**Fig. 5**, green line).

In addition to the feedbacks discussed above, the non-local warming effects on SST lead to a slowdown of the AMOC before the Reforested State is reached (**Fig. A10a**). An increase in SST reduces the density of surface water, leading to stronger ocean stratification and weaker vertical mixing. Moreover, by contributing to the melting of sea ice, the increase in SST leads to an additional freshwater input, further reducing the density of surface water and weakening the vertical mixing in the Labrador Sea. Due to the reduction in the associated meridional heat transport, the AMOC slowdown dampens the temperature increase at high latitudes during that period, slightly counteracting the effects of the water vapor, sea ice-albedo, and temperature-vegetation feedbacks.

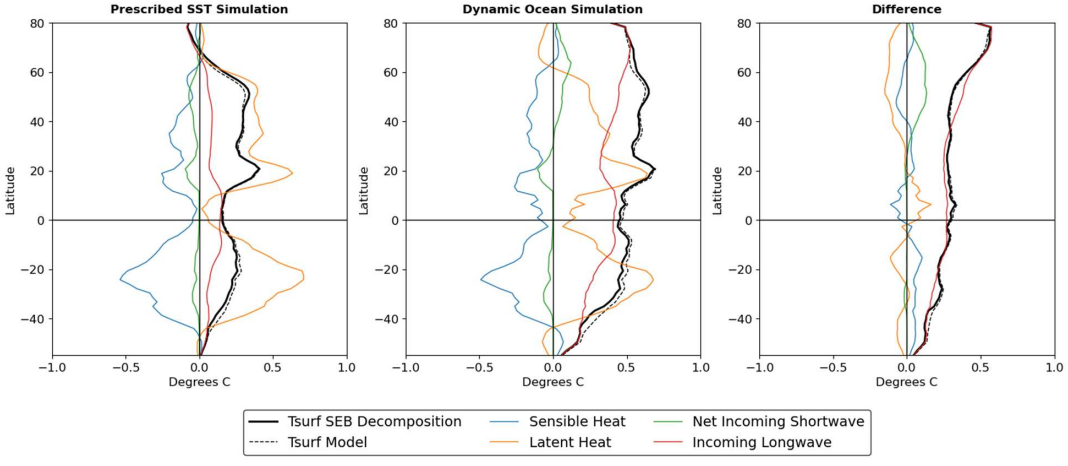

Figure 5: Surface Energy Balance Decomposition of non-local biogeophysical effects over land after reforestation of 50% of grid cells when the Reforested State is reached in the Prescribed SST Simulation and in the Dynamic Ocean Simulation, and difference between the two surface energy balance decompositions (Dynamic Ocean Simulation minus Prescribed SST Simulation).

3.3 Amplification of non-local effects by ocean dynamics increases over time

The non-local warming effects of reforestation lag behind the local effects due to ocean dynamics, continuing to strengthen for multiple centuries after local effects have stabilized. Once the Reforested State is

https://doi.org/10.5194/egusphere-2025-4000
Preprint. Discussion started: 29 September 2025

reached, the local effects have largely stabilized, with minimal further increases, and so have the non-local effects in the Prescribed SST Simulation (**Fig. 6**). However, in the Dynamic Ocean Simulation, the non-local warming effects continue to strengthen for another 500 years, leading to a lag in the non-local response compared to the local response (**Fig. 6**). A similar pattern is observed for T_{air}, where a significant proportion of the total increase in T_{air} is observed in the 500 years following the reach of the Reforested State in the Dynamic Ocean Simulation, whereas there is only a marginal increase during that time period in the Prescribed SST Simulation (**Fig. A10b, A11**).

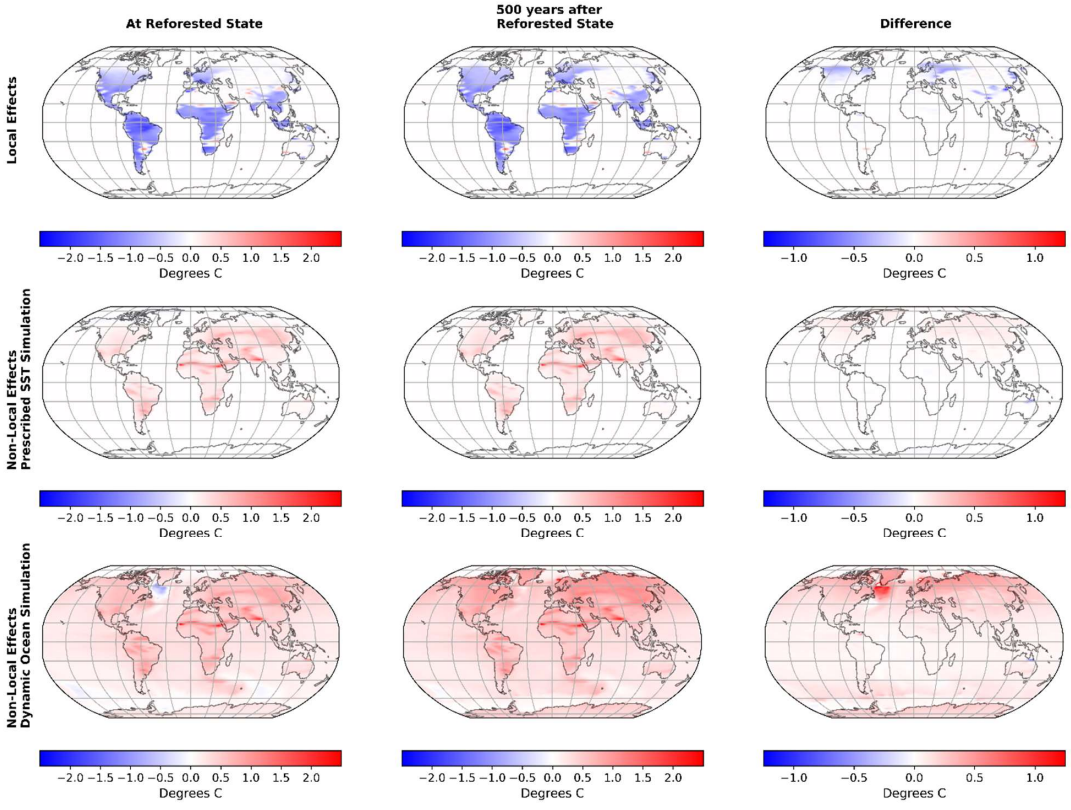

Figure 6: Local, and non-local effects of reforestation of 50% of grid cells on surface temperature (T_{surf_land} and SST) when the Reforested State is reached (left panels), 500 years following the reach of the Reforested State (middle panels), and difference between these two timesteps (right panels) in the Prescribed SST Simulation and in the Dynamic Ocean Simulation. Local effects are identical in the Prescribed SST Simulation and in the Dynamic Ocean Simulation. Maps of local effects show the local effects on reforested grid cells and their interpolation to non-reforested grid cells. Note the difference in color scale between the maps.

This large and steady increase of the non-local warming effect in the Dynamic Ocean Simulation is the result of a gradual increase in SST, which continues to increase even after local effects have stabilized (**Fig. 6**, **A10b**). This is primarily due to the thermal inertia of the ocean combined with amplifying climate feedbacks. The

https://doi.org/10.5194/egusphere-2025-4000
Preprint. Discussion started: 29 September 2025

ocean takes multiple centuries to equilibrate with the atmosphere due to its large heat capacity and slow mixing processes. This slow heat absorption and redistribution sustains a gradual increase in SST over long timescales, continuing even after local effects have stabilized. Moreover, the heat stored in the deep ocean can resurface due to ocean currents or mixing processes, further contributing to a prolonged SST increase. In addition, the AMOC regains strength and almost recovers to its pre-reforestation level 500 years following the reach of the Reforested State (**Fig. A10a**). The increase in meridional heat transport during these 500 years contributes to the greater increase in SST seen at high latitudes in that period (**Fig. 6**). The ongoing increase in SST after local effects have stabilized is amplified by climate feedbacks, such as the water vapor feedback and the sea ice-albedo feedback. This continued increase in SST ultimately leads to further T_{air} and T_{surf_land} warming, as described in the prior section.

This strengthening of the non-local effects over a multi-century period is reflected in the surface energy balance decomposition of the Dynamic Ocean Simulation. The incoming longwave radiation and, to a lesser extent, the net incoming shortwave radiation, continue to increase during the 500-year period following the reach of the Reforested State, particularly at high latitudes due to the processes and feedbacks described previously. In contrast, these components show only minimal increase in the Prescribed SST Simulation over the same period, leading to marginal temperature changes after the Reforested State has been reached (**Fig. 7**, red lines and green lines).

The contribution of ocean dynamics to amplifying non-local warming effects over a multi-century period is not limited to extremely large-scale idealized reforestation experiments. A land cover sensitivity analysis with reforestation of 25% of grid cells (Dynamic Ocean Simulation-25% and Prescribed SST Simulation-25%), more in-line with historical deforestation extent, reveals the same temporal and geographic patterns in non-local warming, but with approximately half of the magnitude. The sensitivity analysis also shows a similar proportion of the non-local warming being driven by ocean dynamics (**Fig. A12, A13**).

https://doi.org/10.5194/egusphere-2025-4000
Preprint. Discussion started: 29 September 2025

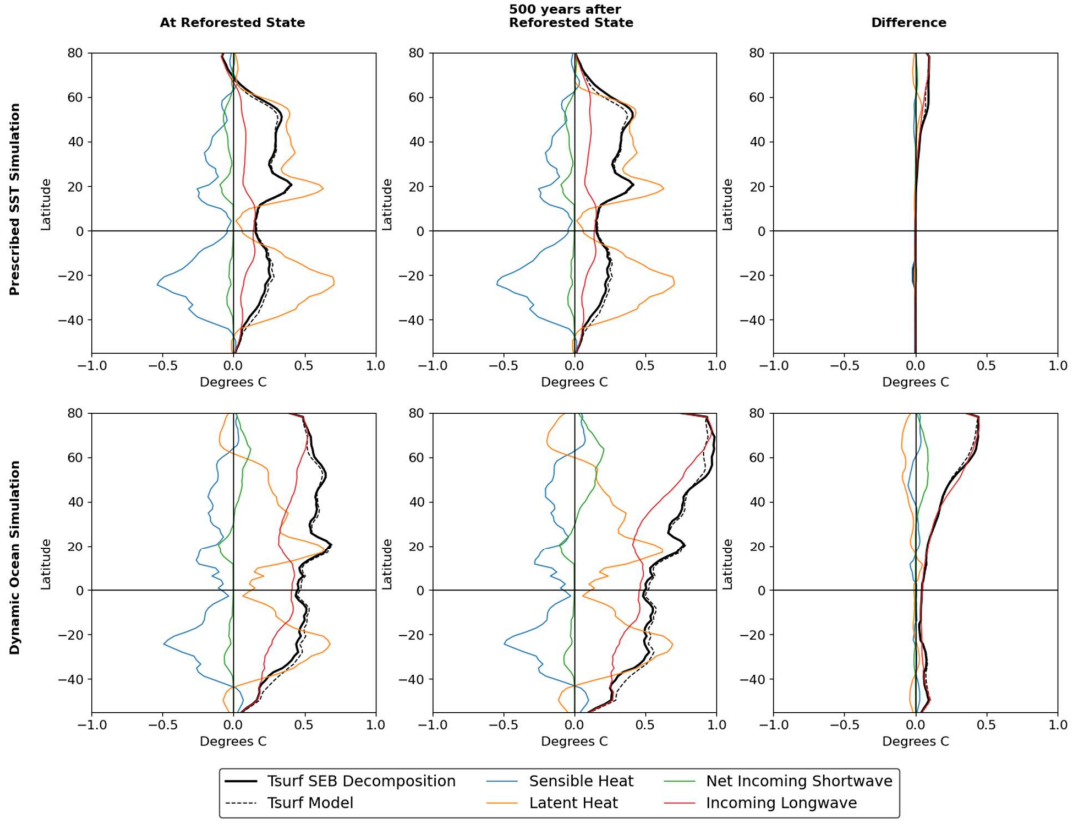

Figure 7: Surface Energy Balance decomposition of the non-local biogeophysical effects over land after reforestation of 50% of grid cells when the Reforested State is reached (left panels), 500 years following the reach of the Reforested State (middle panels), and difference between the two surface energy balance decompositions (right panels), for both the Prescribed SST Simulation and the Dynamic Ocean Simulation.

4. Discussion

In this study, we investigate the role of ocean dynamics on the non-local biogeophysical effects of large-scale forestation using the UVic ESCM. We analyzed the temporal dynamics of the non-local warming effects by comparing results at different points in time over a multi-century period, which had not been done in prior studies. Results show that non-local warming effects driven by ocean dynamics take longer to reach their full extent and continue to strengthen even after forests have regrown and local effects have stabilized. These temporal dynamics of the non-local warming effects suggest that there is a committed warming from the biogeophysical effects of large-scale forestation driven by oceanic thermal inertia. This is analogous to the committed warming from past increases in atmospheric CO_2, assuming CO_2 concentration remains constant going forward, which is also driven by oceanic processes (Wigley, 2005). The full extent of the non-local effects therefore lags behind the local effects. This

https://doi.org/10.5194/egusphere-2025-4000
Preprint. Discussion started: 29 September 2025

committed non-local warming and the resulting differences in the timescale of local and non-local effects must be considered when assessing the full Earth system response of forestation. Large-scale forestation projects that appear beneficial when considering biogeochemical and even local biogeophysical effects may therefore lead to a non-local biogeophysical warming that intensifies over time, undermining their overall effectiveness.

Our results confirm the importance of the non-local warming effects of forestation found in prior studies (Chen et al., 2022; De Hertog et al., 2023; Ma et al., 2013; Wang et al., 2015), while highlighting that ocean dynamics are a key driving mechanism of these non-local effects. The strengthening of ocean-driven non-local warming effects over timescales of centuries may explain the much smaller ocean-driven warming found by Wang et al. (2015) in their study of the seasonal climate impact of Southern Hemisphere forestation. In addition to forestation being limited to the Southern Hemisphere, Wang et al. (2015) used a timeframe of 110 years, compared to 500 years following the reach of the Reforested State in our study. A multi-century timescale is necessary to see the full committed warming from the biogeophysical effects of large-scale forestation.

In addition to influencing the magnitude of the non-local effects, ocean dynamics also influence their geographic distribution, increasing warming significantly more at high latitudes than in the Tropics. This greater increase in non-local warming effects at high latitudes due to ocean dynamics is consistent with prior global studies on deforestation. Davin & Noblet-Ducoudré (2010) found that the ocean mediated cooling resulting from deforestation lowered T_{surf_land} by 1.6K globally, but by 2K at high latitudes. Similarly, Ganopolski et al. (2001) found that the incorporation of a dynamic ocean amplified the T_{air} cooling resulting from boreal deforestation by 0.8K, whereas it added an additional cooling of only 0.5K in the Tropics following tropical deforestation. This reveals the importance of incorporating ocean dynamics when assessing the non-local biogeophysical effects of forestation to obtain an accurate depiction of their spatial distribution. Future research is, however, necessary to determine whether large-scale forestation over different latitudinal bands could lead to different patterns of amplification at high latitudes.

Our results also show that climate feedbacks amplify the committed non-local warming driven by ocean dynamics. Although the trigger of the water vapor feedback and the sea ice-albedo feedback by the ocean's response had been identified in prior studies (Ganopolski et al., 2001; Ma et al., 2013; Wang et al., 2015), no prior studies of large-scale global forestation had performed a surface energy balance decomposition of non-local effects isolating the impact of ocean dynamics. Our surface energy balance decomposition shows a significant increase in incoming longwave radiation resulting from the ocean's response, which, combined with the global increase in specific humidity, reveals the dominant effect of the water vapor feedback in increasing T_{surf_land} at all latitudes, but particularly at high latitudes. This also highlights the role of atmospheric advection in the water vapor feedback over land. Although ocean-atmosphere interactions lead to an increase of moisture in the atmosphere over oceans, atmospheric advection moves this moisture between the ocean and the land surface. This increase in land specific humidity triggered by an increase in SST was also found in other studies (Chadwick et al., 2016). In addition, the surface energy balance decomposition also reveals a slight increase in net incoming shortwave radiation at high latitudes in the Dynamic Ocean Simulation, which can be attributed to the temperature-vegetation feedback at high

https://doi.org/10.5194/egusphere-2025-4000
Preprint. Discussion started: 29 September 2025

latitudes. Although the biophysical warming effect of greening at high latitudes has been established in other studies (Li et al., 2023), this increase in the non-local warming effect of forestation due to Earth greening may not have been seen in other studies of the biogeophysical effects of forestation due to their shorter timeframes.

In the UVic ESCM, the forest regrows globally when starting from a fully deforested state, not reproducing alternative stable states in tropical forests found in other studies (Hirota et al., 2011). It takes approximately 500 years for the Reforested State to be reached due to the slow regrowth of needleleaf trees at high latitudes. This timescale will vary from model to model. While the local effects tend to stabilize when vegetation has regrown, the non-local effects are dependent on the slow timescale of oceanic processes. We therefore expect that in models with a shorter timeframe of forest regrowth, a larger proportion of the non-local effects is realized after vegetation has regrown. In such models, consideration of a multi-century timescale is therefore even more important for capturing the full extent of non-local effects.

Regarding the effects of forestation on the AMOC, the slowdown observed during the timeframe necessary to reach the Reforested state and the formation of a warming hole in the North Atlantic during that period are consistent with prior studies (Portmann et al., 2022; Wang et al., 2014). On the other hand, the recovery observed in the subsequent 500 years had not been observed in prior studies, potentially due to their shorter timeframes. This recovery could be caused by the increase in evapotranspiration over the ocean over time, increasing salinity and density, and favoring ocean mixing. Moreover, an AMOC recovery often follows an AMOC weakening as salty water accumulates at low latitudes and is then transported to high latitudes where it increases salinity and re-intensifies the AMOC. However, further research is necessary to determine the exact causes of such recovery.

Despite consistency with prior studies, there are limitations in performing idealized forestation experiments with the UVic ESCM. Firstly, as mentioned previously, the UVic ESCM does not incorporate cloud feedbacks. Forestation tends to increase low-level cloud coverage locally, most strongly in the Tropics, partially counteracting the decrease in albedo (Cerasoli et al., 2021; Duveiller et al., 2021; Hua et al., 2023; Luo et al., 2024). The non-local effects on clouds are more uncertain, but most models point towards a decrease in non-local cloudiness in mid to high latitudes (De Hertog et al., 2023; Hua et al., 2023). To facilitate comparison with models with a fully dynamic atmosphere, we include a comparison of the surface energy fluxes between the UVic ESCM and CMIP6 models based on a deforestation experiment within the Land Use Model Intercomparison Project (LUMIP) in **Appendix B**. Consideration of cloud feedbacks in our simulations would likely result in a decrease in net shortwave radiation in the Tropics and an increase in net shortwave radiation at high latitudes (**Fig. B2d**). Given the importance of cloud feedbacks on the amount and distribution of water vapor in the atmosphere (Laguë et al., 2023), including cloud feedbacks would also change the strength of the water vapor feedback and hence the incoming longwave radiation, weakening it in the Tropics and strengthening it at high latitudes (**Fig. B2e**). Most models incorporating cloud dynamics show a global T_{surf_land} warming response to forestation driven by a strong non-local warming effect at high latitudes, a similar result to this study (Boysen et al., 2020; De Hertog et al., 2023; Liu et al., 2023). However, many models find a non-local cooling effect in the Tropics driven by atmospheric feedbacks, yet this effect is generally weaker and less widespread than the warming at high latitudes (De Hertog et al., 2023; Liu et al., 2023).

https://doi.org/10.5194/egusphere-2025-4000
Preprint. Discussion started: 29 September 2025

Although it is likely that the amplifying role of the ocean found in this study remains valid in the presence of cloud feedbacks, a tropical non-local cooling would reduce the magnitude of this amplification. Secondly, as mentioned earlier, in the UVic ESCM, forestation leads to a decrease in latent heat flux on land, which is contrary to most models (**Fig. B2a**). However, since the increase in sensible heat flux more than offsets the decrease in latent heat flux, the increase in the total non-radiative flux (sensible heat flux + latent heat flux) is consistent with other models (Boysen et al., 2020; De Hertog et al., 2023). Differences in the latent heat flux over reforested areas should not impact the long-term non-local warming trend found in this study as both latent and sensible heat fluxes contribute to the warming of T_{air}. On the other hand, since evapotranspiration leads to an increase in the water vapor content of the atmosphere, the strength of the water vapor feedback may be impacted. Finally, the idealized large-scale global nature of this study is not meant to reflect global patterns of forestation considered in mitigation pathways. However, the sensitivity analysis performed with a reforestation extent of 25% suggests the presence of a committed non-local warming driven by ocean dynamics approximately proportional to the area subject to forestation. The reforestation threshold at which ocean dynamics lead to a non-negligible committed non-local warming is also an area for future research.

5. Conclusions

Our study suggests that land-based mitigation strategies involving large-scale forestation must consider the complete Earth system response over sufficiently long timeframes to include the slow ocean's response and capture the committed non-local warming. Although biogeochemical effects from CO_2 removal and local biogeophysical effects may occur over relatively short timeframes (Windisch et al., 2021), the full extent of the non-local biogeophysical warming effects may take significantly longer to manifest itself. However, including the full extent of the non-local biogeophysical effects into decision-making frameworks and net-zero policies is challenging. Net-zero policy timeframes are often much shorter than the Earth system's response timeframe. Furthermore, differences across models resulting in spatial variation and uncertainty in the magnitude of these non-local effects complicate their quantification and incorporation into policy considerations. Finally, incorporating long-term warming effects that happen away from forestation sites in national net-zero policies may prove to be politically controversial. In this context, although forestation projects offer numerous benefits in terms of ecosystem services and biodiversity, their use in net-zero policies should be carefully considered. Alternatively, a focus on geological net zero, where a tonne of CO_2 emitted in the atmosphere is offset by a tonne of CO_2 stored in geological reservoirs (Allen et al., 2024; Fankhauser et al., 2022), would avoid issues related to biogeophysical effects and ensure that net-zero policies are in line with achieving climate targets.

https://doi.org/10.5194/egusphere-2025-4000
Preprint. Discussion started: 29 September 2025

Appendix A

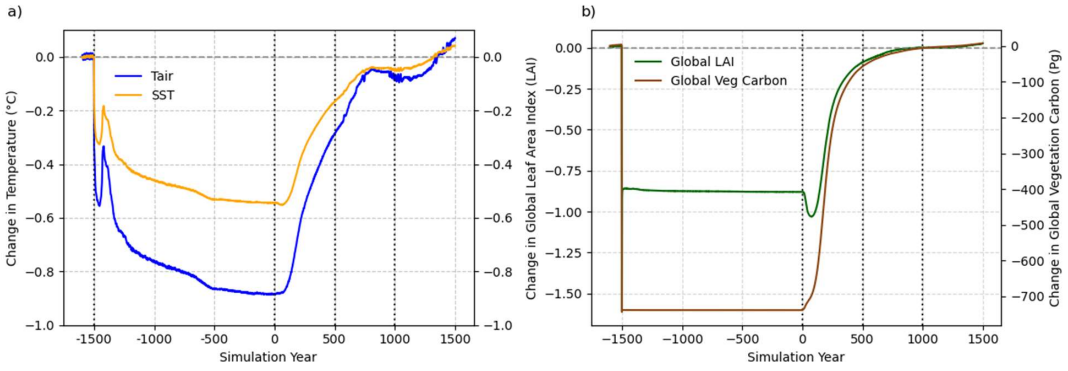

Figure A1: a) Change in T_{air} and SST from the initial spin-up when 100% of grid cells are deforested at simulation year -1500 and subsequently reforested at year 0. b) Change in global Leaf Area Index (combined for all PFTs) and global vegetation carbon (combined for all PFTs) from the initial spin-up when 100% of grid cells are deforested at simulation year -1500 and subsequently reforested at year 0. Year 500 refers to the Reforested State, when the growth of PFTs is stabilizing and vegetation has almost recovered to its pre-deforestation state.

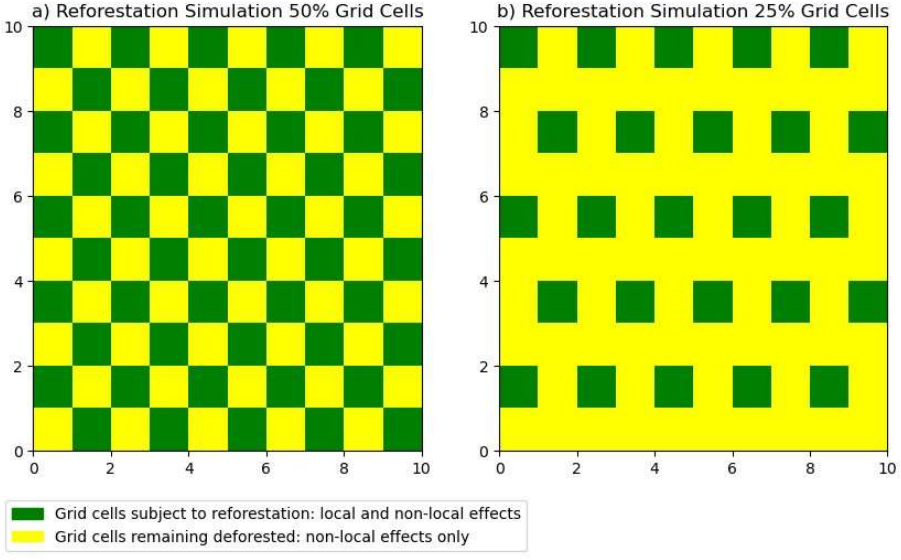

Figure A2: Illustration of the checkerboard approach to reforestation over land grid cells when a) 50% of grid cells are subject to reforestation; and b) 25% of grid cells are subject to reforestation.

https://doi.org/10.5194/egusphere-2025-4000
Preprint. Discussion started: 29 September 2025

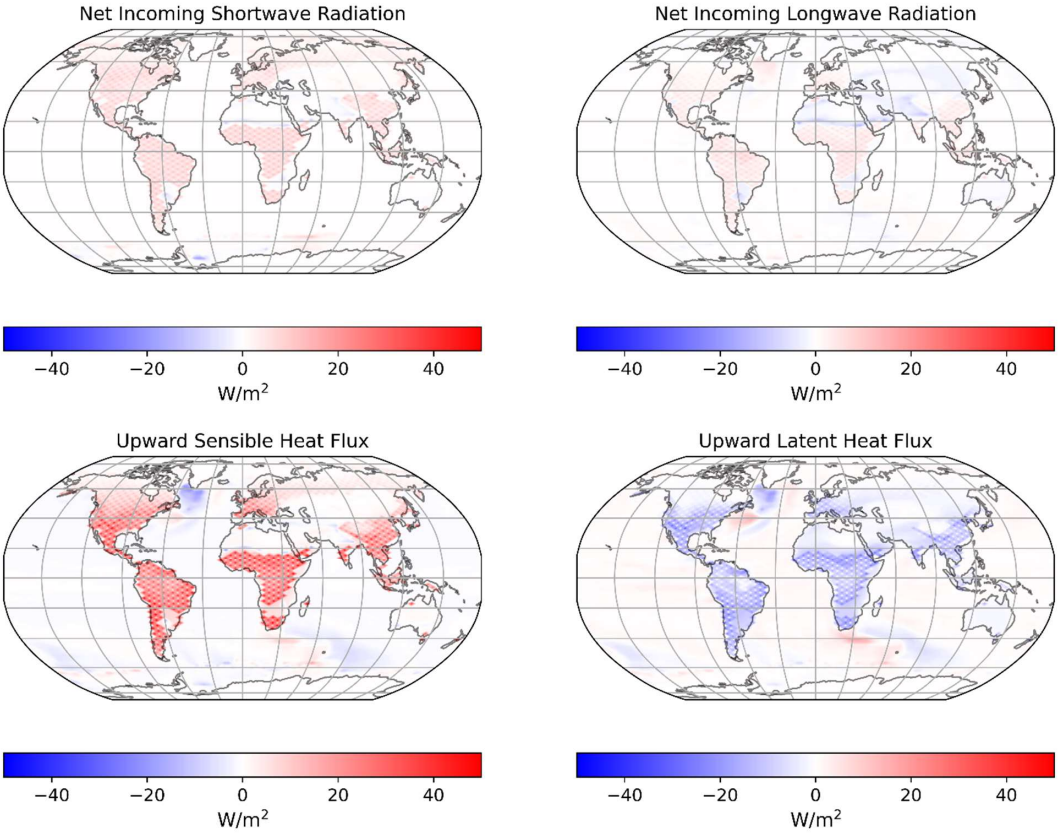

Figure A3: Change in net incoming shortwave radiation, net incoming longwave radiation, upward sensible heat flux and upward latent heat flux between the end of the Deforestation Simulation and when the Reforested State is reached in the Dynamic Ocean Simulation, following reforestation of 50% of grid cells.

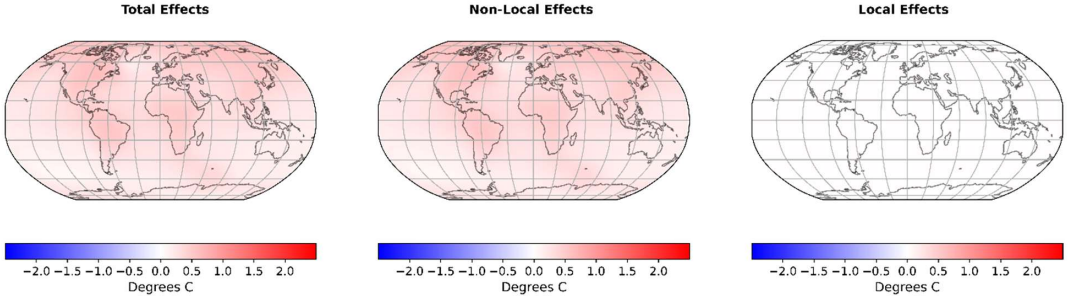

Figure A4: Total, non-local, and local biogeophysical effects of reforestation of 50% of grid cells on Surface Air Temperature (T_{air}) when the Reforested State is reached in the Dynamic Ocean Simulation.

https://doi.org/10.5194/egusphere-2025-4000
Preprint. Discussion started: 29 September 2025

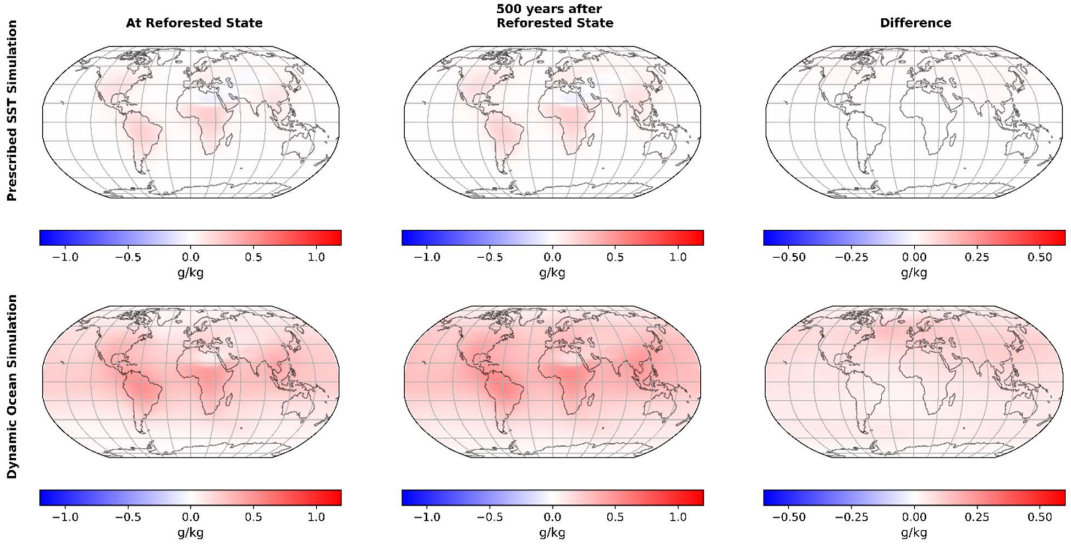

Figure A5: Change in surface specific humidity in g/kg after reforestation of 50% of grid cells when the Reforested State is reached (left panels), 500 years following the reach of the Reforested State (middle panels), and difference between these two timesteps (right panels) in the Prescribed SST Simulation and in the Dynamic Ocean Simulation. Note the difference in color scale between the maps.

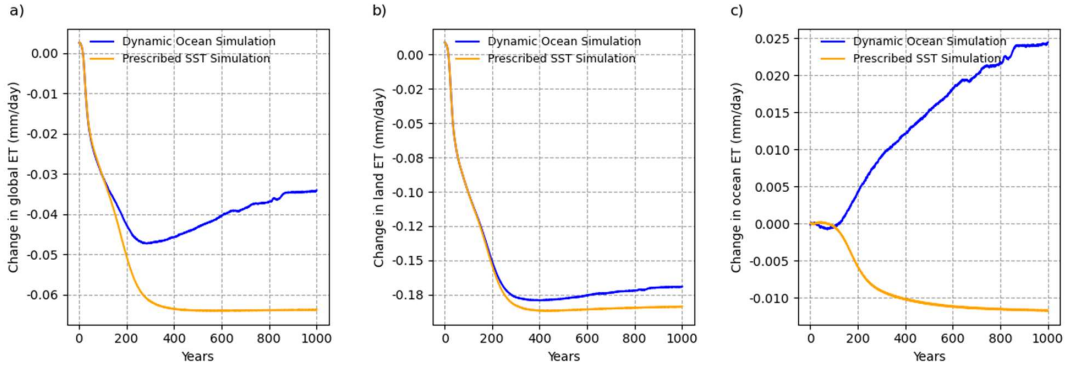

Figure A6: a) Change in global evapotranspiration (ET) over time after reforestation of 50% of grid cells in the Dynamic Ocean Simulation and in the Prescribed SST Simulation b) Change in land ET over time after reforestation of 50% of grid cells in the Dynamic Ocean Simulation and in the Prescribed SST Simulation c) Change in ocean ET over time after reforestation of 50% of grid cells in the Dynamic Ocean Simulation and in the Prescribed SST Simulation.

https://doi.org/10.5194/egusphere-2025-4000
Preprint. Discussion started: 29 September 2025

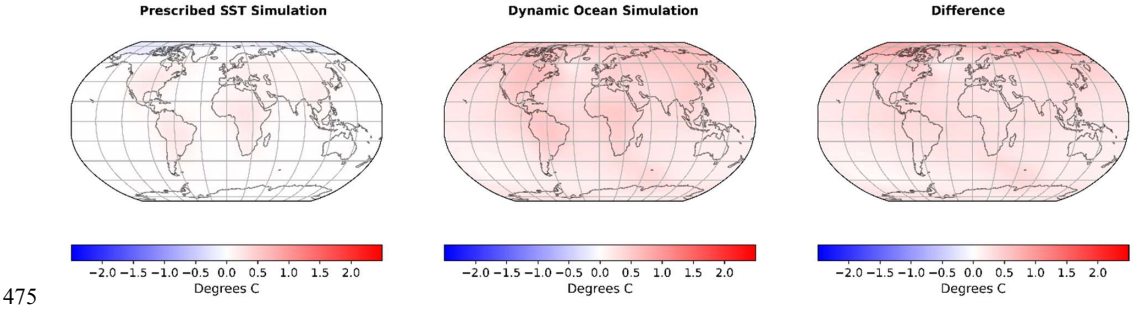

Figure A7: Non-local biogeophysical effects of reforestation of 50% of grid cells on Surface Air Temperature (T_{air}) when the Reforested State is reached in the Prescribed SST Simulation and in the Dynamic Ocean Simulation, and difference between the non-local effects of these two simulations.

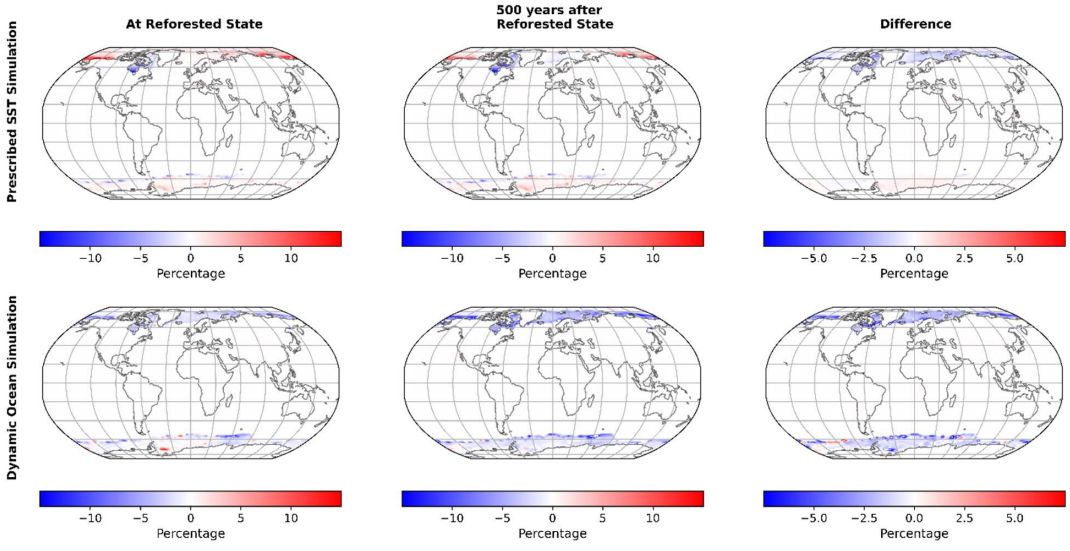

Figure A8: Change in percent of grid cell covered by sea ice after reforestation of 50% of grid cells when the Reforested State is reached (left panels), 500 years following the reach of the Reforested State (middle panels), and difference between these two timesteps (right panels) in the Prescribed SST Simulation and in the Dynamic Ocean Simulation. Note the difference in color scale between the maps.

https://doi.org/10.5194/egusphere-2025-4000
Preprint. Discussion started: 29 September 2025

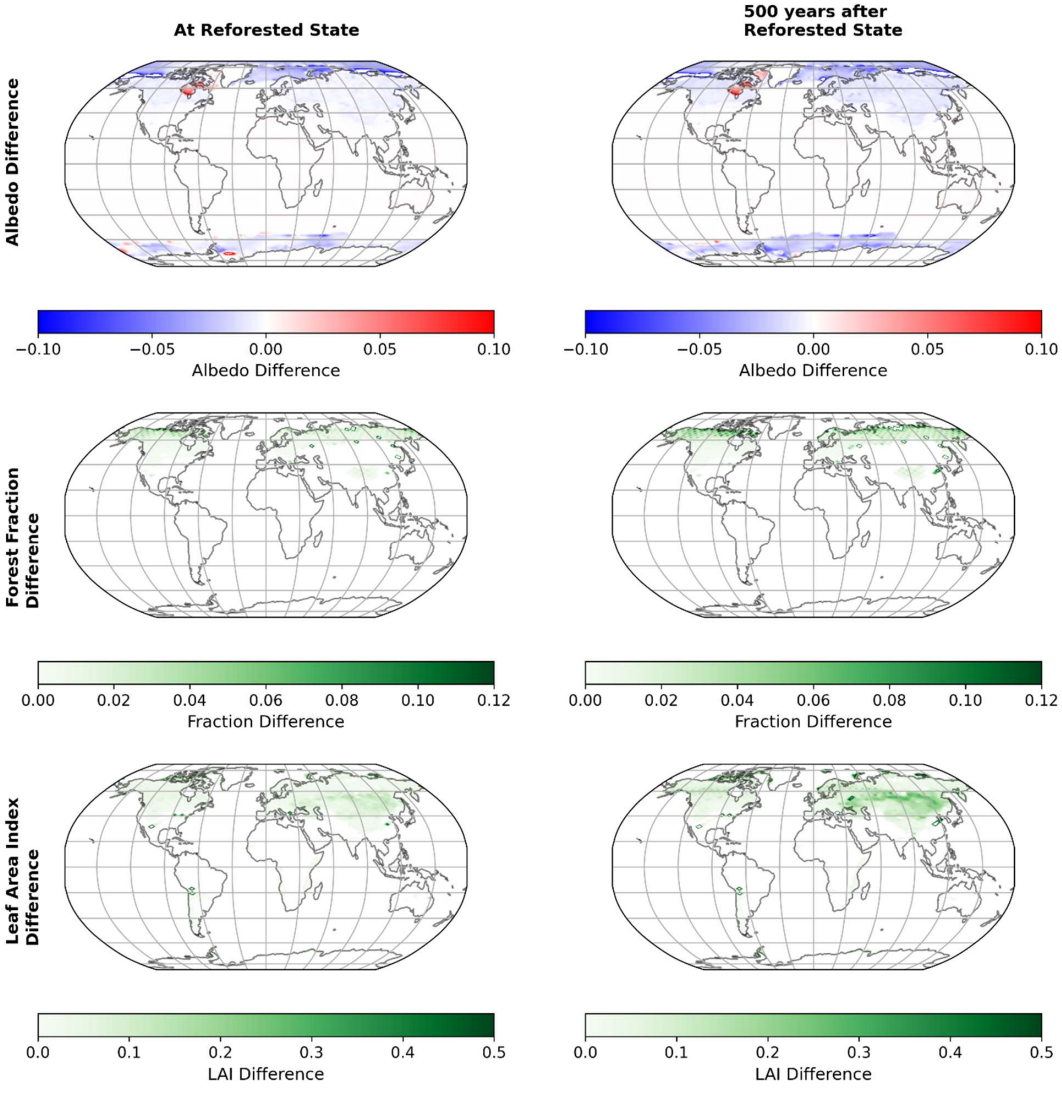

485 **Figure A9:** Difference between the Dynamic Ocean Simulation and the Prescribed SST Simulation in albedo, fraction of grid cell covered by forest (shrubs, broadleaf trees, and needleleaf trees), and LAI for all PFTs combined, when the Reforested State is reached and 500 years following the reach of the Reforested State.

https://doi.org/10.5194/egusphere-2025-4000
Preprint. Discussion started: 29 September 2025

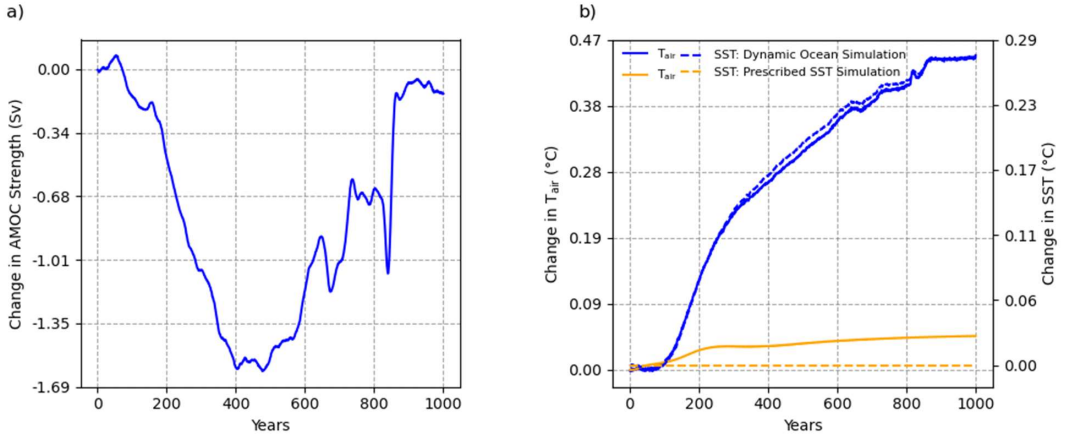

Figure A10: a) Change in the strength of the meridional overturning circulation following reforestation of 50% of grid cells b) Change in Surface Air Temperature (T_{air}) and SST over time following reforestation of 50% of grid cells in the Dynamic Ocean Simulation (blue) and in the Prescribed SST Simulation (orange).

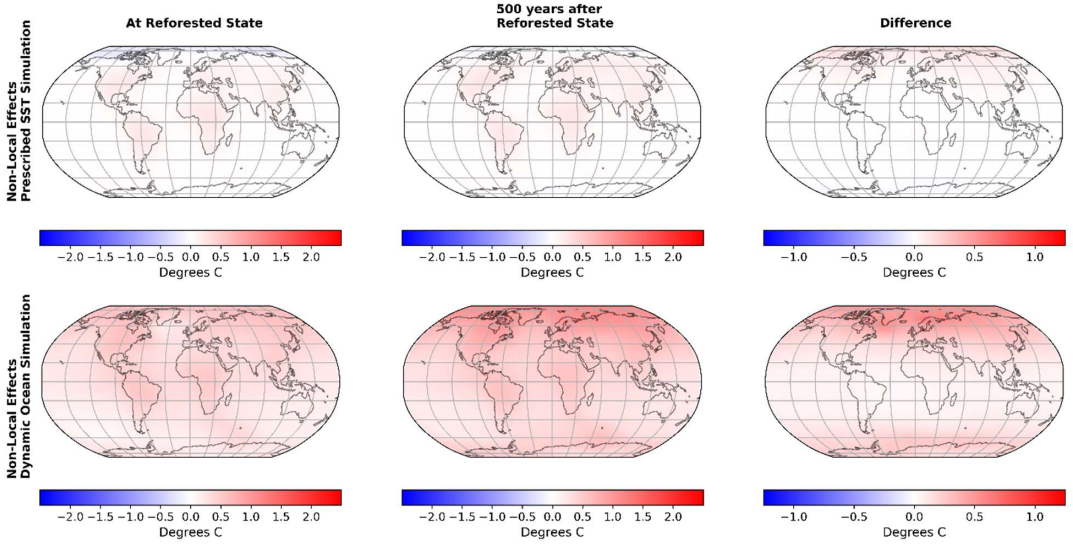

Figure A11: Non-local effects of reforestation of 50% of grid cells on Surface Air Temperature (T_{air}) when the Reforested State is reached (left panels), 500 years following the reach of the Reforested State (middle panels), and difference between these two timesteps (right panels) in the Prescribed SST Simulation and in the Dynamic Ocean Simulation. Note the difference in color scale between the maps.

https://doi.org/10.5194/egusphere-2025-4000
Preprint. Discussion started: 29 September 2025

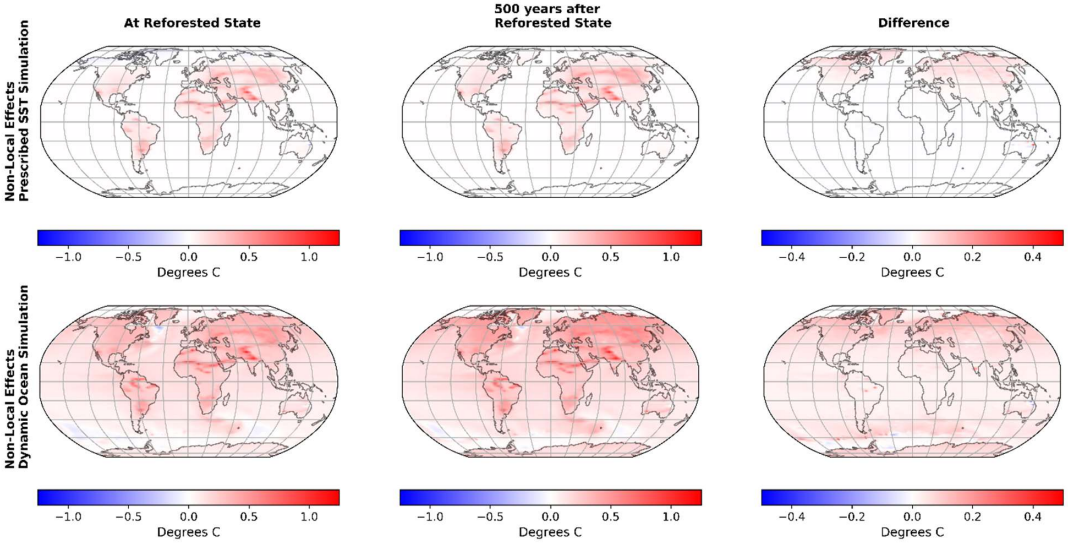

Figure A12: Non-local effects of reforestation of 25% of grid cells on surface temperature (T_{surf_land} and SST) when the Reforested State is reached (left panels), 500 years following the reach of the Reforested State (middle panels), and difference between these two timesteps (right panels) in the Prescribed SST Simulation and in the Dynamic Ocean Simulation. Note the difference in color scale between the maps.

https://doi.org/10.5194/egusphere-2025-4000
Preprint. Discussion started: 29 September 2025

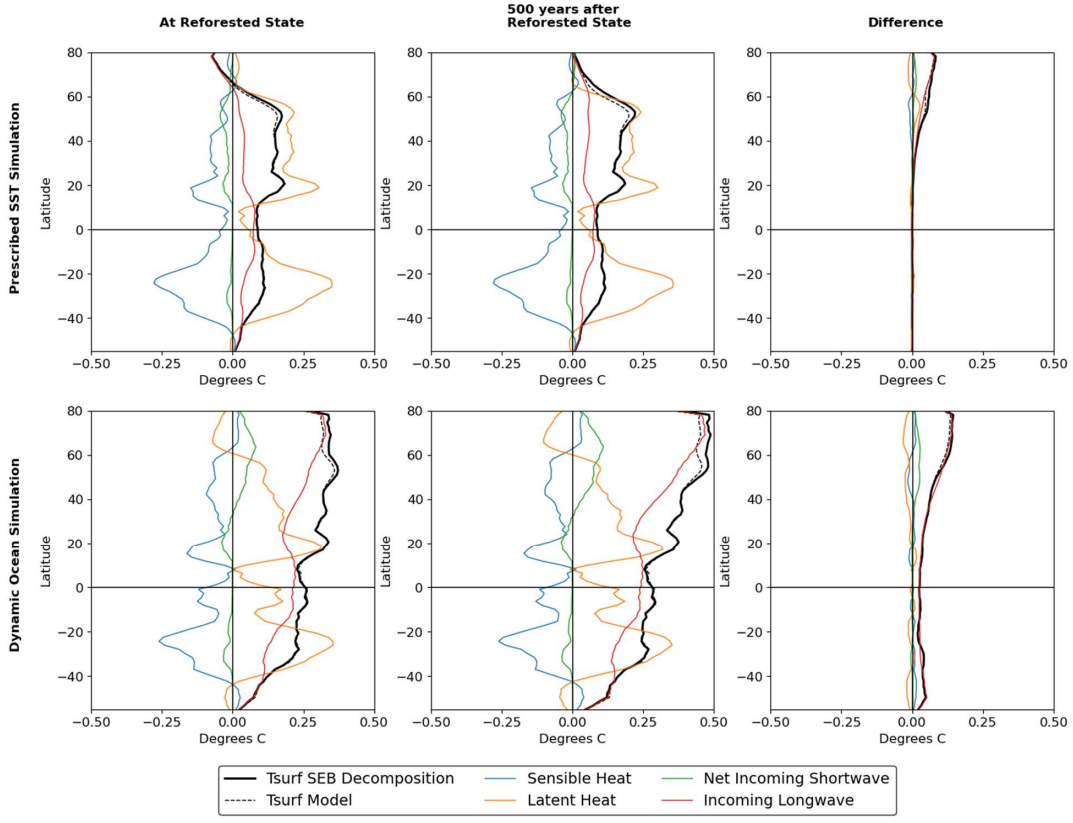

Figure A13: Surface Energy Balance decomposition of the non-local biogeophysical effects over land after reforestation of 25% of grid cells when the Reforested State is reached (left panels), 500 years following the reach of the Reforested State (middle panels), and difference between the two surface energy balance decompositions (right panels), for both the Prescribed SST Simulation and the Dynamic Ocean Simulation.

Appendix B

Below, we present the results of the analysis of the biogeophysical effects of deforestation in the UVic ESCM following the *deforest-glob* experiment described in Lawrence et al. (2016) organized under the Land-use Model Intercomparison Project (LUMIP). The *deforest-glob* experiment prepared with the UVic ESCM didn't result in the full 20M km^2 of forest area removed by 1900 (and even 1950), resulting in a smaller deforested area at high latitudes compared to other models, as per **Fig. B1**. The surface energy balance analysis follows the methodology described in Boysen et al. (2020) to allow for a comparison of the UVic ESCM with CMIP6 models, with the exception that the mean of the years 1940-1950 as opposed to 1895-1905 was used to obtain a stronger signal for each parameter. It is important to note that the smaller extent of deforestation at high latitudes in the UVic ESCM at least partially explains the weaker signal seen at high latitudes in the UVic ESCM compared to CMIP6 models.

https://doi.org/10.5194/egusphere-2025-4000
Preprint. Discussion started: 29 September 2025

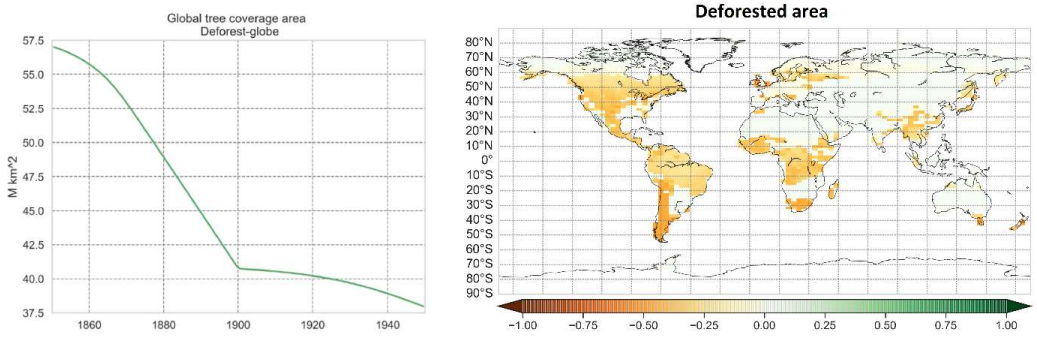

Figure B1: Change in global tree coverage area between 1850 and 1950 in the *deforest-glob* experiment in the UVic ESCM (left panel) and fraction of grid cell deforested by 1950 (right panel).

https://doi.org/10.5194/egusphere-2025-4000
Preprint. Discussion started: 29 September 2025

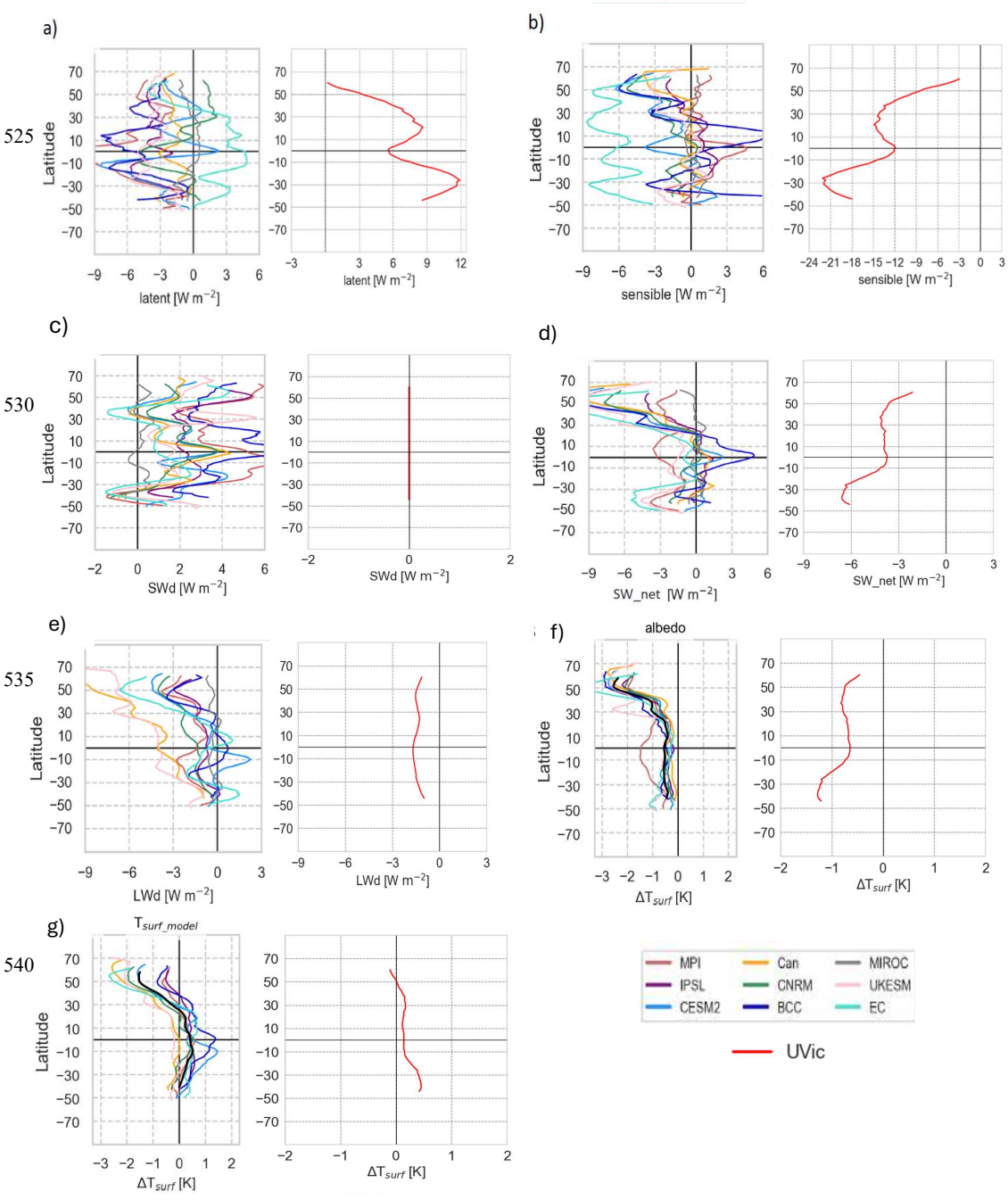

Figure B2: Comparison of the changes in zonally averaged surface energy fluxes following the *deforest-glob* experiment (including only areas of deforestation) between the CMIP6 models and the UVic ESCM. CMIP6 model comparison figures come from Boysen et al. (2020). a) latent heat flux b) sensible heat flux c) downward shortwave

https://doi.org/10.5194/egusphere-2025-4000
Preprint. Discussion started: 29 September 2025

radiation d) net downward shortwave radiation e) downward longwave radiation f) surface albedo g) land surface temperature. An approximated running mean over 10° latitude was applied to smooth lines.

Data and Code availability

The model code for version 2.10 of the UVic ESCM is available on the official UVic ESCM webpage at https://terra.seos.uvic.ca/model/2.10/. Model output as well as code to perform the analysis and generate the figures are available to editors and reviewers upon request and will be made available in a public repository upon publication.

Author contribution

PEB and KZ conceived the study; PEB and KZ designed the experiments; PEB and AJM performed model simulations; PEB conducted the analysis and wrote the initial manuscript; all co-authors contributed to the interpretation of results and to the final version.

Competing interests

PEB and AJM declare no competing interests. KZ is an editor for the journal *Earth System Dynamics*.

Acknowledgements

This research was enabled in part by support provided by BC Digital Research Infrastructure and the Digital Research Alliance of Canada. We also thank Marzieh Mortezapour for assisting in the preparation of the deforestation comparison with other models provided in Appendix B.

Financial Support

This project was undertaken with the financial support of the Government of Canada. Ce projet a été realisé avec l'appui financier du Gouvernement du Canada. PEB acknowledges support from the Natural Sciences and Engineering Research Council of Canada's Undergraduate Student Research Award program.

https://doi.org/10.5194/egusphere-2025-4000
Preprint. Discussion started: 29 September 2025

References

Allen, M. R., Frame, D. J., Friedlingstein, P., Gillett, N. P., Grassi, G., Gregory, J. M., Hare, W., House, J., Huntingford, C., Jenkins, S., Jones, C. D., Knutti, R., Lowe, J. A., Matthews, H. D., Meinshausen, M., Meinshausen, N., Peters, G. P., Plattner, G.-K., Raper, S., Rogelj, J., Stott, P. A., Solomon, S., Stocker, T. F., Weaver, A. J., and Zickfeld, K.: Geological Net Zero and the need for disaggregated accounting for carbon sinks, Nature, 1–3, https://doi.org/10.1038/s41586-024-08326-8, 2024.

Arora, V. K. and Montenegro, A.: Small temperature benefits provided by realistic afforestation efforts, Nature Geosci, 4, 514–518, https://doi.org/10.1038/ngeo1182, 2011.

Betts, R. A.: Offset of the potential carbon sink from boreal forestation by decreases in surface albedo, Nature, 408, 187–190, https://doi.org/10.1038/35041545, 2000.

Betts, R. A., Falloon, P. D., Goldewijk, K. K., and Ramankutty, N.: Biogeophysical effects of land use on climate: Model simulations of radiative forcing and large-scale temperature change, Agricultural and Forest Meteorology, 142, 216–233, https://doi.org/10.1016/j.agrformet.2006.08.021, 2007.

Bitz, C. M., Holland, M. M., Weaver, A. J., and Eby, M.: Simulating the ice-thickness distribution in a coupled climate model, Journal of Geophysical Research: Oceans, 106, 2441–2463, https://doi.org/10.1029/1999JC000113, 2001.

Bonan, G. B.: Forests and Climate Change: Forcings, Feedbacks, and the Climate Benefits of Forests, Science, https://doi.org/10.1126/science.1155121, 2008.

Boysen, L. R., Brovkin, V., Pongratz, J., Lawrence, D. M., Lawrence, P., Vuichard, N., Peylin, P., Liddicoat, S., Hajima, T., Zhang, Y., Rocher, M., Delire, C., Séférian, R., Arora, V. K., Nieradzik, L., Anthoni, P., Thiery, W., Laguë, M. M., Lawrence, D., and Lo, M.-H.: Global climate response to idealized deforestation in CMIP6 models, Biogeosciences, 17, 5615–5638, https://doi.org/10.5194/bg-17-5615-2020, 2020.

Buckley, M. W. and Marshall, J.: Observations, inferences, and mechanisms of the Atlantic Meridional Overturning Circulation: A review, Reviews of Geophysics, 54, 5–63, https://doi.org/10.1002/2015RG000493, 2016.

Cerasoli, S., Yin, J., and Porporato, A.: Cloud cooling effects of afforestation and reforestation at midlatitudes, Proc. Natl. Acad. Sci. U.S.A., 118, e2026241118, https://doi.org/10.1073/pnas.2026241118, 2021.

Chadwick, R., Good, P., and Willett, K.: A Simple Moisture Advection Model of Specific Humidity Change over Land in Response to SST Warming, Journal of Climate, 29, 7613–7632, 2016.

Chen, C., Ge, J., Guo, W., Cao, Y., Liu, Y., Luo, X., and Yang, L.: The Biophysical Impacts of Idealized Afforestation on Surface Temperature in China: Local and Nonlocal Effects, Journal of Climate, 35, 7833–7852, https://doi.org/10.1175/JCLI-D-22-0144.1, 2022.

Chen, L. and Dirmeyer, P. A.: Reconciling the disagreement between observed and simulated temperature responses to deforestation, Nat Commun, 11, 202, https://doi.org/10.1038/s41467-019-14017-0, 2020.

Cook-Patton, S. C., Leavitt, S. M., Gibbs, D., Harris, N. L., Lister, K., Anderson-Teixeira, K. J., Briggs, R. D., Chazdon, R. L., Crowther, T. W., Ellis, P. W., Griscom, H. P., Herrmann, V., Holl, K. D., Houghton, R. A., Larrosa, C., Lomax, G., Lucas, R., Madsen, P., Malhi, Y., Paquette, A., Parker, J. D., Paul, K., Routh, D., Roxburgh, S., Saatchi, S., van den Hoogen, J., Walker, W. S., Wheeler, C. E., Wood, S. A., Xu, L., and

https://doi.org/10.5194/egusphere-2025-4000
Preprint. Discussion started: 29 September 2025

Griscom, B. W.: Mapping carbon accumulation potential from global natural forest regrowth, Nature, 585, 545–550, https://doi.org/10.1038/s41586-020-2686-x, 2020.

Cox, P.: Description of the TRIFFID dynamic global vegetation model, Hadley Centre Technical Note, 24, 2001.

Davin, E. L. and Noblet-Ducoudré, N. de: Climatic Impact of Global-Scale Deforestation: Radiative versus Nonradiative Processes, Journal of Climate, 23, 97–112, https://doi.org/10.1175/2009JCLI3102.1, 2010.

De Hertog, S. J., Havermann, F., Vanderkelen, I., Guo, S., Luo, F., Manola, I., Coumou, D., Davin, E. L., Duveiller, G., Lejeune, Q., Pongratz, J., Schleussner, C.-F., Seneviratne, S. I., and Thiery, W.: The biogeophysical effects of idealized land cover and land management changes in Earth system models, Earth System Dynamics, 14, 629–667, https://doi.org/10.5194/esd-14-629-2023, 2023.

Devaraju, N., Noblet-Ducoudré, N. de, Quesada, B., and Bala, G.: Quantifying the Relative Importance of Direct and Indirect Biophysical Effects of Deforestation on Surface Temperature and Teleconnections, Journal of Climate, 31, 3811–3829, https://doi.org/10.1175/JCLI-D-17-0563.1, 2018.

Duveiller, G., Filipponi, F., Ceglar, A., Bojanowski, J., Alkama, R., and Cescatti, A.: Revealing the widespread potential of forests to increase low level cloud cover, Nat Commun, 12, 4337, https://doi.org/10.1038/s41467-021-24551-5, 2021.

Eyring, V., Bony, S., Meehl, G. A., Senior, C. A., Stevens, B., Stouffer, R. J., and Taylor, K. E.: Overview of the Coupled Model Intercomparison Project Phase 6 (CMIP6) experimental design and organization, Geoscientific Model Development, 9, 1937–1958, https://doi.org/10.5194/gmd-9-1937-2016, 2016.

Fankhauser, S., Smith, S. M., Allen, M., Axelsson, K., Hale, T., Hepburn, C., Kendall, J. M., Khosla, R., Lezaun, J., Mitchell-Larson, E., Obersteiner, M., Rajamani, L., Rickaby, R., Seddon, N., and Wetzer, T.: The meaning of net zero and how to get it right, Nat. Clim. Chang., 12, 15–21, https://doi.org/10.1038/s41558-021-01245-w, 2022.

Ganopolski, A., Petoukhov, V., Rahmstorf, S., Brovkin, V., Claussen, M., Eliseev, A., and Kubatzki, C.: CLIMBER-2: a climate system model of intermediate complexity. Part II: model sensitivity, Climate Dynamics, 17, 735–751, https://doi.org/10.1007/s003820000144, 2001.

Hirota, M., Holmgren, M., Van Nes, E. H., and Scheffer, M.: Global Resilience of Tropical Forest and Savanna to Critical Transitions, Science, 334, 232–235, https://doi.org/10.1126/science.1210657, 2011.

Hua, W., Zhou, L., Dai, A., Chen, H., and Liu, Y.: Important non-local effects of deforestation on cloud cover changes in CMIP6 models, Environ. Res. Lett., 18, 094047, https://doi.org/10.1088/1748-9326/acf232, 2023.

Laguë, M. M., Quetin, G. R., and Boos, W. R.: Reduced terrestrial evaporation increases atmospheric water vapor by generating cloud feedbacks, Environ. Res. Lett., 18, 074021, https://doi.org/10.1088/1748-9326/acdbe1, 2023.

Lawrence, D. M., Hurtt, G. C., Arneth, A., Brovkin, V., Calvin, K. V., Jones, A. D., Jones, C. D., Lawrence, P. J., de Noblet-Ducoudré, N., Pongratz, J., Seneviratne, S. I., and Shevliakova, E.: The Land Use Model Intercomparison Project (LUMIP) contribution to CMIP6: rationale and experimental design, Geoscientific Model Development, 9, 2973–2998, https://doi.org/10.5194/gmd-9-2973-2016, 2016.

https://doi.org/10.5194/egusphere-2025-4000
Preprint. Discussion started: 29 September 2025

Li, C., von Storch, J.-S., and Marotzke, J.: Deep-ocean heat uptake and equilibrium climate response, Clim Dyn, 40, 1071–1086, https://doi.org/10.1007/s00382-012-1350-z, 2013.

Li, Y., Li, Z.-L., Wu, H., Zhou, C., Liu, X., Leng, P., Yang, P., Wu, W., Tang, R., Shang, G.-F., and Ma, L.: Biophysical impacts of earth greening can substantially mitigate regional land surface temperature warming, Nat Commun, 14, 1–12, https://doi.org/10.1038/s41467-023-35799-4, 2023.

Liu, S., Hua, W., Zhou, L., Chen, H., Yu, M., Li, X., and Cui, Y.: Local and Non-Local Biophysical Impacts of Deforestation on Global Temperature During Boreal Summer: CMIP6-LUMIP Multimodel Analysis, JGR Atmospheres, 128, e2022JD038229, https://doi.org/10.1029/2022JD038229, 2023.

Liu, W., Fedorov, A. V., Xie, S.-P., and Hu, S.: Climate impacts of a weakened Atlantic Meridional Overturning Circulation in a warming climate, Science Advances, 6, eaaz4876, https://doi.org/10.1126/sciadv.aaz4876, 2020.

Luo, H., Quaas, J., and Han, Y.: Decreased cloud cover partially offsets the cooling effects of surface albedo change due to deforestation, Nat Commun, 15, 7345, https://doi.org/10.1038/s41467-024-51783-y, 2024.

Ma, D., Notaro, M., Liu, Z., Chen, G., and Liu, Y.: Simulated impacts of afforestation in East China monsoon region as modulated by ocean variability, Clim Dyn, 41, 2439–2450, https://doi.org/10.1007/s00382-012-1592-9, 2013.

MacDougall, A. H. and Knutti, R.: Projecting the release of carbon from permafrost soils using a perturbed parameter ensemble modelling approach, Biogeosciences, 13, 2123–2136, https://doi.org/10.5194/bg-13-2123-2016, 2016.

Macdougall, A. H., Avis, C., and Weaver, A.: Significant contribution to climate warming from the permafrost carbon feedback, Nature Geoscience, 5, https://doi.org/10.1038/NGEO1573, 2012.

Mengis, N., Keller, D. P., MacDougall, A. H., Eby, M., Wright, N., Meissner, K. J., Oschlies, A., Schmittner, A., MacIsaac, A. J., Matthews, H. D., and Zickfeld, K.: Evaluation of the University of Victoria Earth System Climate Model version 2.10 (UVic ESCM 2.10), Geoscientific Model Development, 13, 4183–4204, https://doi.org/10.5194/gmd-13-4183-2020, 2020.

Minx, J. C., Lamb, W. F., Callaghan, M. W., Fuss, S., Hilaire, J., Creutzig, F., Amann, T., Beringer, T., De Oliveira Garcia, W., Hartmann, J., Khanna, T., Lenzi, D., Luderer, G., Nemet, G. F., Rogelj, J., Smith, P., Vicente Vicente, J. L., Wilcox, J., and Del Mar Zamora Dominguez, M.: Negative emissions—Part 1: Research landscape and synthesis, Environ. Res. Lett., 13, 063001, https://doi.org/10.1088/1748-9326/aabf9b, 2018.

Mo, L., Zohner, C. M., Reich, P. B., Liang, J., de Miguel, S., Nabuurs, G.-J., Renner, S. S., van den Hoogen, J., Araza, A., Herold, M., Mirzagholi, L., Ma, H., Averill, C., Phillips, O. L., Gamarra, J. G. P., Hordijk, I., Routh, D., Abegg, M., Adou Yao, Y. C., Alberti, G., Almeyda Zambrano, A. M., Alvarado, B. V., Alvarez-Dávila, E., Alvarez-Loayza, P., Alves, L. F., Amaral, I., Ammer, C., Antón-Fernández, C., Araujo-Murakami, A., Arroyo, L., Avitabile, V., Aymard, G. A., Baker, T. R., Bałazy, R., Banki, O., Barroso, J. G., Bastian, M. L., Bastin, J.-F., Birigazzi, L., Birnbaum, P., Bitariho, R., Boeckx, P., Bongers, F., Bouriaud, O., Brancalion, P. H. S., Brandl, S., Brearley, F. Q., Brienen, R., Broadbent, E. N., Bruelheide, H., Bussotti, F., Cazzolla Gatti, R., César, R. G., Cesljar, G., Chazdon, R. L., Chen, H. Y. H., Chisholm, C., Cho, H.,

https://doi.org/10.5194/egusphere-2025-4000
Preprint. Discussion started: 29 September 2025

Cienciala, E., Clark, C., Clark, D., Colletta, G. D., Coomes, D. A., Cornejo Valverde, F., Corral-Rivas, J. J., Crim, P. M., Cumming, J. R., Dayanandan, S., de Gasper, A. L., Decuyper, M., Derroire, G., DeVries, B., Djordjevic, I., Dolezal, J., Dourdain, A., Engone Obiang, N. L., Enquist, B. J., Eyre, T. J., Fandohan, A. B., Fayle, T. M., Feldpausch, T. R., Ferreira, L. V., Finér, L., Fischer, M., Fletcher, C., Frizzera, L., Gianelle, D., Glick, H. B., Harris, D. J., Hector, A., Hemp, A., Hengeveld, G., Hérault, B., Herbohn, J. L., Hillers, A., Honorio Coronado, E. N., Hui, C., Ibanez, T., Imai, N., et al.: Integrated global assessment of the natural forest carbon potential, Nature, 624, 92–101, https://doi.org/10.1038/s41586-023-06723-z, 2023.

Noblet-Ducoudré, N. de, Boisier, J.-P., Pitman, A., Bonan, G. B., Brovkin, V., Cruz, F., Delire, C., Gayler, V., Hurk, B. J. J. M. van den, Lawrence, P. J., Molen, M. K. van der, Müller, C., Reick, C. H., Strengers, B. J., and Voldoire, A.: Determining Robust Impacts of Land-Use-Induced Land Cover Changes on Surface Climate over North America and Eurasia: Results from the First Set of LUCID Experiments, Journal of Climate, 25, 3261–3281, https://doi.org/10.1175/JCLI-D-11-00338.1, 2012.

Pongratz, J., Schwingshackl, C., Bultan, S., Obermeier, W., Havermann, F., and Guo, S.: Land Use Effects on Climate: Current State, Recent Progress, and Emerging Topics, Curr Clim Change Rep, 7, 99–120, https://doi.org/10.1007/s40641-021-00178-y, 2021.

Portmann, R., Beyerle, U., Davin, E., Fischer, E. M., De Hertog, S., and Schemm, S.: Global forestation and deforestation affect remote climate via adjusted atmosphere and ocean circulation, Nat Commun, 13, 5569, https://doi.org/10.1038/s41467-022-33279-9, 2022.

Riahi, K., Schaeffer, R., Arango, J., Calvin, K., Guivarch, C., Hasegawa, T., Jiang, K., Kriegler, E., Matthews, R., Peters, G. P., Rao, A., Robertson, S., Sebbit, A. M., Steinberger, J., Tavoni, M., and van Vuuren, D. P.: Mitigation pathways compatible with long-term goals, in: IPCC, 2022: Climate Change 2022: Mitigation of Climate Change. Contribution of Working Group III to the Sixth Assessment Report of the Intergovernmental Panel on Climate Change, Cambridge University Press, Cambridge, UK and New York, NY, USA, 2022.

Roe, S., Streck, C., Obersteiner, M., Frank, S., Griscom, B., Drouet, L., Fricko, O., Gusti, M., Harris, N., Hasegawa, T., Hausfather, Z., Havlík, P., House, J., Nabuurs, G.-J., Popp, A., Sánchez, M. J. S., Sanderman, J., Smith, P., Stehfest, E., and Lawrence, D.: Contribution of the land sector to a 1.5 °C world, Nat. Clim. Chang., 9, 817–828, https://doi.org/10.1038/s41558-019-0591-9, 2019.

Sewell, A., Van Der Esch, S., and Löwenhardt, H.: Goals and Commitments for the Restoration decade: A Global Overview of Countries' Restoration Commitments Under the Rio Conventions and Other Pledges, PBL Netherlands Environmental Assessment Agency, The Hague, 2020.

Smith, H. B., Vaughan, N. E., and Forster, J.: Long-term national climate strategies bet on forests and soils to reach net-zero, Commun Earth Environ, 3, 305, https://doi.org/10.1038/s43247-022-00636-x, 2022.

Smith, P., Davis, S. J., Creutzig, F., Fuss, S., Minx, J., Gabrielle, B., Kato, E., Jackson, R. B., Cowie, A., Kriegler, E., van Vuuren, D. P., Rogelj, J., Ciais, P., Milne, J., Canadell, J. G., McCollum, D., Peters, G., Andrew, R., Krey, V., Shrestha, G., Friedlingstein, P., Gasser, T., Grübler, A., Heidug, W. K., Jonas, M., Jones, C. D., Kraxner, F., Littleton, E., Lowe, J., Moreira, J. R., Nakicenovic, N., Obersteiner, M., Patwardhan, A.,

https://doi.org/10.5194/egusphere-2025-4000
Preprint. Discussion started: 29 September 2025

Rogner, M., Rubin, E., Sharifi, A., Torvanger, A., Yamagata, Y., Edmonds, J., and Yongsung, C.: Biophysical and economic limits to negative CO2 emissions, Nature Clim Change, 6, 42–50, https://doi.org/10.1038/nclimate2870, 2016.

Wang, Y., Yan, X., and Wang, Z.: The biogeophysical effects of extreme afforestation in modeling future climate, Theor Appl Climatol, 118, 511–521, https://doi.org/10.1007/s00704-013-1085-8, 2014.

Wang, Y., Yan, X., and Wang, Z.: Global warming caused by afforestation in the Southern Hemisphere, Ecological Indicators, 52, 371–378, https://doi.org/10.1016/j.ecolind.2014.12.004, 2015.

Weaver, A. J., Eby, M., Wiebe, E. C., Bitz, C. M., Duffy, P. B., Ewen, T. L., Fanning, A. F., Holland, M. M., MacFadyen, A., Matthews, H. D., Meissner, K. J., Saenko, O., Schmittner, A., Wang, H., and Yoshimori, M.: The UVic earth system climate model: Model description, climatology, and applications to past, present and future climates, Atmosphere-Ocean, 39, 361–428, https://doi.org/10.1080/07055900.2001.9649686, 2001.

Weaver, A. J., Sedláček, J., Eby, M., Alexander, K., Crespin, E., Fichefet, T., Philippon-Berthier, G., Joos, F., Kawamiya, M., Matsumoto, K., Steinacher, M., Tachiiri, K., Tokos, K., Yoshimori, M., and Zickfeld, K.: Stability of the Atlantic meridional overturning circulation: A model intercomparison, Geophysical Research Letters, 39, https://doi.org/10.1029/2012GL053763, 2012.

Wigley, T. M. L.: The Climate Change Commitment, Science, 307, 1766–1769, https://doi.org/10.1126/science.1103934, 2005.

Winckler, J., Reick, C. H., and Pongratz, J.: Robust Identification of Local Biogeophysical Effects of Land-Cover Change in a Global Climate Model, Journal of Climate, 30, 1159–1176, https://doi.org/10.1175/JCLI-D-16-0067.1, 2017.

Winckler, J., Reick, C. H., Bright, R. M., and Pongratz, J.: Importance of Surface Roughness for the Local Biogeophysical Effects of Deforestation, J. Geophys. Res. Atmos., 124, 8605–8618, https://doi.org/10.1029/2018JD030127, 2019a.

Winckler, J., Lejeune, Q., Reick, C. H., and Pongratz, J.: Nonlocal Effects Dominate the Global Mean Surface Temperature Response to the Biogeophysical Effects of Deforestation, Geophys. Res. Lett., 46, 745–755, https://doi.org/10.1029/2018GL080211, 2019b.

Windisch, M. G., Davin, E. L., and Seneviratne, S. I.: Prioritizing forestation based on biogeochemical and local biogeophysical impacts, Nat. Clim. Chang., 11, 867–871, https://doi.org/10.1038/s41558-021-01161-z, 2021.

Zickfeld, K., MacIsaac, A. J., Canadell, J. G., Fuss, S., Jackson, R. B., Jones, C. D., Lohila, A., Matthews, H. D., Peters, G. P., Rogelj, J., and Zaehle, S.: Net-zero approaches must consider Earth system impacts to achieve climate goals, Nat. Clim. Chang., 13, 1298–1305, https://doi.org/10.1038/s41558-023-01862-7, 2023.